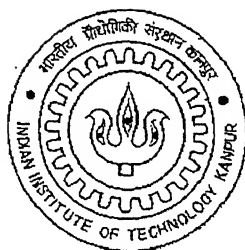# Removal of volatile organic compound by activated carbon fiber (ACF)
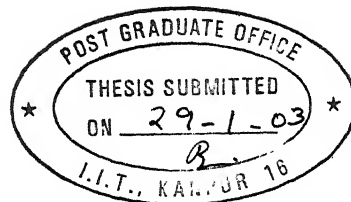
A thesis submitted

in partial fulfillment of the requirements

for the degree of

Master of Technology

by

Debasish Das

to the
Department of Chemical Engineering

INDIAN INSTITUTE OF TECHNOLOGY

KANPUR

February, 2003

CERTIFICATE

It is certified that the work contained in the thesis entitled *Removal of volatile organic compound by activated carbon fiber (ACF)* by **Debasish Das**, has been carried out under my supervision and that this work has not been submitted elsewhere for a degree.

February, 2003

Dr. Nishith Verma

Assistant Professor

Department of Chemical Engineering

Indian Institute of Technology

Kanpur

ABSTRACT

Despite a huge technological advancement, air pollution remains one of the major problems in today's world. Atmosphere is polluted by different gaseous species such as NO_x (NO & NO_2), SO_2, CO, and volatile organic compounds (VOCs) etc. VOCs (e.g. benzene, toluene, and dichloromethane) have recently received greater attention in the field of environmental control due to its primary as well as secondary harmful impacts on ground air quality and human health. Due to its high BET surface area, activated carbon fiber (ACF) has been considered in recent times to be one of the promising adsorbents for controlling VOCs at low concentration level.

In this work, an experimental set-up was designed and developed to carry out dynamic adsorption/desorption study on the removal of toluene at low concentration levels (< 1 % volume concentration) on the ACF wrapped over perforated teflon made reactor. The extent of removal of toluene was studied under various operating conditions such as, bed temperature (35-100 °C), gas inlet concentration (2000-10000 ppm), gas flow rate (0.2-1.0 slpm) and weight of the adsorbent (2-10 gm). A mathematical model was developed to predict the VOC breakthrough characteristics under these operating conditions. The model incorporates the effects of gas film mass transfer coefficient, pore diffusion and the adsorption/desorption rates within the pore.

The experimental results showed that a bed temperature of 50 ^{0}C was most favorable for capturing toluene vapor from nitrogen stream. In a typical adsorption experiments carried out on 5 g of ACF sample the breakthrough and total adsorption times were found to be 7 and 50 min, respectively. The results also showed that the adsorption method was effective if the VOC emission levels were low i.e. parts per millions (ppm). The activated carbon fiber repeatedly showed a good regeneration capability on DC electrical regeneration. The experimental results and the corresponding simulated results from the model developed in this study were compared and found to be in good agreement.

Acknowledgement

At the very beginning I would like to thank **the authority of IIT, Kanpur** for providing high-class facilities and the ambience necessary to carry out research work.

During the research work, my thesis guide **Dr. N. Verma** has helped me immensely with his ingenious ideas and valuable guidance. I am highly grateful to him for motivating and encouraging me during all the stages of my thesis work. By working under his aegis I have come to know the intricate details of research work. His guidance will act as beacon of light throughout my life.

I shall always cherish the sweet memories attached with my lab mates, **Vivek, Satish, Amit, Arun, Ritesh, Kaushal and Akshika**. They have always helped to maintain a friendly atmosphere in our lab. More than this, they have always been a constant source of inspiration.

A thank is due to **Mr. Shivshankar, Rohit** and **Mr. Narendra** for their help.

The time spent with **Tirtha, Jyoti, Saurav, Samui, Shayan, Braja, Giri, AP, Mrinal, Gargi, Arpan, Liton, Partha, Arindam, Chat, Prakash, Dulal, Swarnendu, Asit, and Manojit** in **G-top** and **H-top** has been a major recreation for me. The memories associated with them will surely be cherished forever. During last few days, when the struggle to complete the thesis work was at its peak, mid-night tea parties used to bring a lease of relieve.

Apart from getting help from each and every corner, I want to mention especially about **Kanu, Jyotida, Saurav** and **Tirtha** who acted like real friends, shared my emotions, understood me psychologically and rendered all possible help so that I could live a healthy mental life.

At the end I would like to convey my regards to my **parents** and all other **family members**. Their silent presence behind my all achievements cannot be properly expressed.

February, 2003   Debasish Das

CONTENTS

List of Tables

List of Figures

NOMENCLATURE

a   = External surface area per unit volume of the fiber (1/m)

$a^{\oplus}$ = Total adsorption surface area per unit volume of the fiber (1/m)

C   = Concentration, mol/m^3

C_G = Interfiber concentration of the species, at any arbitrary location r in the bed, (mol/m^2)

C_p = Molar concentration of species at a location r inside the pores, (mol/m^2)

C_s = Molar surface concentration of adsorbed species inside the pores, (mol/m^2)

D_e = Effective diffusivity inside pore, m^2/s,

D_f = Diameter of the fiber, m

D_k = Knudsen diffusivity, m^2/s

D_m = Molecular diffusivity, m^2/s

D_R = Radial dispersion coefficient, m^2/s

k_m = Average mass film transfer coefficient around the fiber, (m/s)

k_a = Rate constant for adsorption, (m/s)

k_d = Rate constant for desorption, $(moles/s-m^2)$

L_{bed} = Length of the bed, m

M   = Molecular weight of gas, gm/g mol

N_r = Molar diffusional flux of the component in the radial direction, $mol/m^2.s$

P   = Pressure, N/m^2

Q   = Volumetric flow rate of the gas, slpm

R   = Universal gas constant, J/kg-K

R_1 = Inner radius of the bed, m

R_2 = Outer radius of the bed, m

R_p = Pore radius, m

Re   = Reynolds Number, $\dfrac{\rho v D_f}{\mu}$

Sc   = Schmidt Number, $\dfrac{\mu}{\rho D_f}$

Sh   = Sherwood Number, $\dfrac{K_m D_f}{D_m}$

T   = Temperature, K

t   = time, sec

V_R = Gas velocity in the radial direction, m/s

Greek Letter

ε = Porosity of bed

α = Porosity of fiber

ρ = Gas density, kg/m^3

μ = Gas viscosity, Pa.s

Subscripts

1   = inner

2   = Outer

max   = Maximum

P   = Pore of the fiber

a   = Adsorption

d   = Desorption

R   = Radial direction of the bed

r   = Radial direction of the pore of the fiber

Superscripts

s   At the fiber outer surface

—   Volume average quatities inside the pores of particle

*   Non-dimensionalized variables

CHAPTER-1
INTRODUCTION

Despite a huge technological advancement, air pollution remains one of the major problems in today's world. Unhealthy air means unhealthy people. Air pollution has an enormous impact on everyone's health, happiness and even the economy. Air is polluted by different gaseous species such as NO_x (NO & NO_2), SO_2, CO, suspended particulate matters (SPM) and volatile organic compounds (VOCs) etc. VOCs (e.g. benzene, toluene, dichloromethane, and trichloroethylene) have recently received greater attention in the field of environmental control.

Why? Emissions of VOCs have primary as well as secondary harmful impacts on ground air quality and human health. Eye, nose and throat irritation, headache, damage to liver and central nervous system, all may occur due to prolonged exposure to VOCs. VOCs may also have carcinogenic effects. Some of these organics can cause cancer in animals; some are suspected or known to cause cancer in humans. The role of VOCs as a precursor in the formation of photochemical smog and a number of toxic byproducts is well established. In atmospheric NOx-O_3-photochemical chemistry, formation of hydroxyl $(OH\bullet)$ radicals is believed to be the main cause of chain reactions leading to the formation of O_3. Atmospheric hydrocarbons and CO further aggravate the chain reactions leading to the formation of extra $OH \bullet$ radicals, which in turn produce extra O_3 and many secondary byproducts such as HNO_3 (source of acid rain), Peroxy acetyl nitrate (PAN) etc. The main steps involved in a typical NOx-O_3-CO photochemical reaction are as follow:

$$NO_2 + h\upsilon \rightarrow NO + O$$
$$O + O_2 + M \rightarrow O_3 + M$$
$$O_3 + NO \rightarrow NO_2 + O$$

$$O_3 + h\upsilon \rightarrow O(^1D)$$
$$O(^1D) + H_2O \rightarrow 2OH \bullet$$
$$CO + OH\bullet \rightarrow CO_2 + HO_2 \bullet$$

$$HO_2 \bullet + NO \rightarrow NO_2(source of excess O_3) + OH \bullet$$
$$OH \bullet + NO_2 \rightarrow HNO_3(By-products)$$
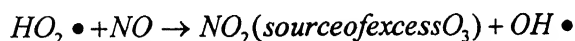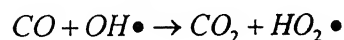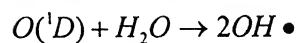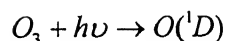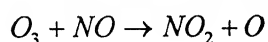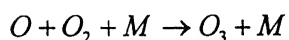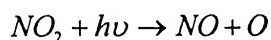
What are the sources? In general, we can divide the sources into two categories: (a) stationary and (b) mobile. Organic chemicals such as solvents, thinners, degreasers, lubricants, and also liquid fuels are used and produced in many chemical industries. During handling, storage, and distribution of these chemicals, a significant amount of VOCs is emitted into atmosphere. VOCs can also be emitted from heating ventilation and air conditioning (HVAC) system (Wolkoff, 1995; Fanger *et al*, 1998) and bacterial and fungal activities (Rivers *et al*, 1992; Batterman *et al*, 1991). The extensive use of petrochemicals based organics and bio-organics in building products results in elevated indoor concentrations of VOCs. It has been seen that aliphatic and olefinic aldehydes and aliphatic acids are emitted from a large number of flooring materials, e.g. rubber, carpets, linoleum and vinyl (Wolkoff, 1995). Few polymeric materials like poly vinyl chloride (PVC) may also emit various types of VOCs.

How to control? The VOCs emission control is presently one of the major activities in environmental program. Various control measures are taken by many industrialized countries to limit VOCs emissions into atmosphere within permitted levels. The commonly emitted VOCs in the atmosphere and the respective permitted emissions levels are listed in Table 1. There are various type of VOCs control methods presently available, including condensation, adsorption, catalytic oxidation and thermal oxidation, etc. (Zesis, B., 1997). The adsorption of VOCs onto porous adsorbents, such as activated carbons, has been suggested as an innovative treatment process. Adsorption has been increasingly utilized in bulk separation or purification processes. The methods (especially condensation), other than adsorption are effective when VOCs concentrations are at higher levels (> 1%). However adsorption has been found to be suitable and economical if VOCs concentrations are at low levels i.e. parts per million (ppm) or sub ppm. Condensation followed by adsorption is found to be more effective if concentration of VOCs vary over a wide range (Verma & Gupta, 2001). Beside this, regeneration is a problem in other processes, however, in the case of adsorption; thermal regeneration is relatively easier to carry out.

The keyword of an adsorption process is a porous solid medium. A high surface area or high micropore volume can be achieved due to the porous structure of solid and thus high adsorptive capacity. Steric, equilibrium and kinetic mechanism are three distinct mechanisms for the adsorption process. In steric mechanism the dimension of the pores is such that, all but the larger molecules can enter into the pores. In equilibrium mechanism, stronger adsorbing species is preferentially removed by the

solid. The different rates of diffusion of different species into the pore are the main parameters in kinetic mechanism. Thus, faster diffusing species is preferentially removed by the solid. The success or failure of the process depends on how the solids perform in both equilibria and kinetics. A solid exhibiting good adsorptive capacity as well as faster kinetics is supposed to be a good adsorbent. Therefore in order to be a good adsorbent, a solid must have (a) reasonably high surface area or micropore volume and (b) relatively larger pore network for the transport of molecules to the interior.

There are various adsorbents commonly used in industries such as alumina, silica gel, GAC (granular activated carbon) and zeolites, etc. These days, activated carbon fiber (ACF) has been considered to be one of the promising adsorbents for controlling VOCs at low concentration level. Due to its high BET surface area and pore size distribution (micropore volume), the adsorption capacity of ACF is higher than any other adsorbents. Pressure drop in the bed is an important factor. If the adsorbents are in powder (powder activated carbon, PAC) or granular (GAC) form, pressure drop in the bed is high, which is not desirable in industries. Regeneration is off course another important factor. In the case of ACF, regeneration can be done at a temperature of 150^0C & at a lower flow rate, whereas a high temperature ($350-400^0C$) and gas flow rate are required for the regeneration of GAC. ACF in bundled form becomes lighter and even stronger than steel. Carbon fiber is highly resistant to abrasion and chemical corrosion, and provides good lubricity. Not only as an adsorbent, ACF can also be used as catalyst supports, electrical and electronic materials for its unique pore structures and useful levels of electrical conductivity. Though it is a most complex solid, but due to its extremely high surface area and micropore volume it has been preferred by most of the industries. ACFs are synthesized from various homogenous polymeric base materials (precursors), such as poly acrylonitrile (PAN), phenolic resins, cellulose derivatives, and coal tar pitch [Mochida, 2000]. The essential microstructure of ACFs is developed during carbonization followed by activation of precursor materials by partial gasification in steam and/or CO_2. The development of the microstructure is influenced by many factors, including the types of activating agent and operating conditions for carbonization and activation. Carbonization is essentially a de-volatilizing step to create pores within the materials. The subsequent step, activation causes the

development of a pore size distribution (PSD) and specific surface area responsible for adsorption.

Following the introductory part and objectives, a review of the work done so far on the removal of VOC by adsorption on ACF by different investigators is discussed in the second chapter. A detailed description of the theoretical analysis and mathematical model, to understand the mechanism of the process is discussed in the third chapter. A description of the experimental set up is given in the fourth chapter. The fifth chapter describes the experimental results, along with the validation of the model developed. The conclusion drawn from the present work and scope of the future work have been presented in the sixth chapter

1.1 Objectives

The objectives of this thesis work are as follows:

1) Design and set-up of an experimental test bench to study adsorption and desorptipon characteristics for the removal of VOCs on ACF.

2) Determine breakthrough characteristics of the materials under varying operating conditions such as bed temperature, concentrations of VOCs, gas flow rate and weight of ACF, on the removal of VOCs.

3) Study the effects of different operating conditions (bed temperature and concentrations of VOCs) on the removal of VOCs by two different samples of ACFs, one synthesized from viscous rayon & other from PAN (procured from abroad).

4) Determine the optimal adsorption temperature and heat of adsorption for removal of VOCs on ACF.

5) Carry out theoretical analysis and development of a mathematical model for the adsorption of VOCs on ACF, to understand the adsorption mechanism and to predict the breakthrough characteristics.

6) Model verification with the experimental data.

CHAPTER 2
LITERATURE SURVEY

This chapter presents a critical review of various works done on the adsorption of VOCs by ACFs, together with different theoretical models developed to understand the mechanism of the removal process. An attempt has been made to identify the areas, which require further study. A review of various studies on the VOC adsorption by ACF reveals that most of the works may be categorized mainly in three groups: (1) equilibrium study to explain the isotherm data, (2) investigation of the effects of various operating conditions on the adsorption capacity of ACF for VOCs, such as temperature, concentration, etc. and (3) study to determine the breakthrough characteristics of VOCs on ACF under dynamic condition.

Rood et al. (1994) have studied experimentally and theoretically, the equilibrium adsorption capacities of ACFs for acetone or benzene in air. The adsorption isotherms were measured and corresponding model equations were proposed for the ACF samples having three different BET surface areas. The concentration levels for the adsorbates chosen ranged between 10 and 1000 ppmv. The adsorption isotherm model proposed by Dubinin and Freundlich were used to fit the isotherm data. Dubinin-Redushkevich (DR) equation is one of the many equations developed by Dubinin to describe equilibrium adsorption of gaseous adsorbates. The equation is as follows:

$\ln W = \ln W_0 - (x_0 / \beta k)^2 A^2$; where W and x_0 are the volumes adsorbed per unit mass of adsorbent [cm^3/g] and slit-pore half-width [nm] respectively A good agreement between the model prediction and experimental data using the DR equation was achieved for both acetone and benzene. It was concluded for both the adsorbates that ACFs with the smaller slit pore half widths (related to lower BET surface areas) were more effective adsorbents than ACFs with larger mean pore sizes (higher BET surface area) at low adsorbate concentration levels (10-200 ppmv).

Do et al. (1998) have studied a pure-component equilibrium adsorption isotherm of methane, ethane, and propane at different temperatures. The binary adsorption of methane in two heavier hydrocarbons (ethane and propane) by activated carbons having different pore structures were also studied. Six models were applied to the single and binary experimental data, namely: ideal adsorption solution theory (IAST), isoteric heat as a function of loading model (IHFL), micropore-size distribution

(MPSD), energy distribution (ED), and extended Langmuir and Sips models. IAST (Myers and Prausnitz, 1965) is based on a sound thermodynamic framework and widely used as a standard for multicomponent equilibria. In IHFL (Do and Do, 1997) model the variation of isoteric heat with loading is regarded as the measure of the heterogeneity of the adsorbent. This general model was tested with the single component adsorption isotherm data of many adsorbates on different samples of activated carbon and zeolites with good success. The MPSD model is based on the assumption that the surface heterogeneity of activated carbon is induced by the size distribution of the slit-shaped micropores. Sips (Sips, 1948) isotherm model is a combination of the Langmuir and Freundlich equations. This three parameter equation has been widely used for fitting the isotherm data of different hydrocarbons on activated carbon. It was found that all six models worked with a reasonably good accuracy to describe the experimental data of the hydrocarbon on commercial activated carbon.

Verma and Dasgupta (2002) have studied the removal of VOCs from a gaseous mixture by cryogenic condensation, adsorption and a process combining both. Mathematical models were developed to predict the extent of removal of a binary mixture of VOCs in air by these two methods. The model developed to predict the breakthrough characteristics of VOCs consisted of an unsteady state species balance in the bulk gas phase, within the pores and on the surface of the adsorbing material. The kinetic rate expressions for the adsorption and desorption were obtained from the Sips equation. The Sips equation was obtained by equating the adsorption and the desorption rate. It was found that the Sips isotherm was suitable in explaining the isothermal adsorption/desorption behavior of a binary mixture of di-methyl chloride (DMC) and toluene. The model developed, was applied to simulate the experimental breakthrough curves reported elsewhere for the adsorption of various binary mixtures of organic compounds by activated carbon (Yun et al. 1999).

In the following section a review on the effects of different operating conditions on the adsorption capacity of ACF for the removal of VOCs has been presented.

Cal et al. (1995) have studied the effects of relative humidity (RH) on the adsorption of water soluble (acetone) and water insoluble (benzene) VOCs on activated carbon cloth (ACC). The RH values from 0-90% and organic concentrations from 350-1000 ppmv were examined. It was found that the presence of water vapor in the gas stream did not have appreciable effects on the adsorption of 500 ppmv

benzene until about 65% RH, when a rapid decrease resulted in benzene adsorption capacity with increasing RH. It was concluded that at the higher RH capillary condensation of water vapor occurred within the ACC pores, making them unavailable for benzene adsorption. It was also found that increase in benzene concentration might have a significant effect on the amount of water vapor adsorbed. At 86% RH and 500 ppmv, 284 mg water per g of ACC was adsorbed, while at 86% RH and 1000 ppmv, only 165 mg/g of water was adsorbed. It was also concluded that lower the benzene concentration the more profound the effect of water vapor on the adsorption capacity of ACC. The presence of water vapor in the gas stream with acetone had little effect on the adsorption capacity even at RHs of 90%. This is most likely because acetone is infinitely soluble in water, whereas benzene is insoluble and hydrophobic.

Suyadal et al. (2000) have investigated the dynamic adsorption of trichloroethylene (TCE) in a laboratory scale packed-bed adsorber (PBA) on activated carbon at constant pressure (101.3 kPa). The experiments were carried out at different temperatures (25.6 ^{0}C $\leq$ T $\leq$ 35.8 ^{0}C) and with the TCE feedstock concentrations levels between 6300 and 8000 ppm. It was observed that TCE breakthrough curve shifted towards the left (short breakthrough time) with an increase in feedstock concentration. This behavior indicated a much quicker saturation of the adsorbent at higher concentration level. A shift in TCE breakthrough curve towards the right was also observed with decrease in temperature, which was attributed to an increase in the amount of adsorbed TCE. However no adsorption isotherm was proposed to fit the adsorption data

Kang et al. (2001) have studied the adsorption behavior of polar methyl-ethyl-ketone (MEK) and non-polar benzene vapors on the viscous rayon-based activated carbon fibers in order to investigate the dependence of adsorption on adsorbate polarity. The influence of adsorbate polarity on the adsorption capacity and dynamic adsorption and desorption characteristics was studied. For polar MEK, it was found that a larger specific area resulted in a greater adsorption capacity if the concentration was greater than 100 ppm. However, reverse was the case when the concentration was less than 100 ppm. A larger specific surface area resulted in a higher adsorption capacity for non-polar benzene over the entire experimental range. The results also show that the adsorption capacity of MEK was greater than that of benzene for ACF with lower surface area. On the contrary, the adsorption capacity of

7

MEK was lower than that of benzene for ACF with larger surface area. It was concluded that the effect of adsorbate polarity on the adsorption capacity was more significant in the case of adsorbents with a smaller surface area. The time to reach equilibrium was much longer (2400 min) for non-polar benzene, whereas the time for MEK was only 1200 min. It was concluded that there was considerable oxygen complexes on the ACF surface, which had a greater affinity for the polar adsorbates and hence hastened the adsorption process. The desorption behavior of ACF with higher surface area was also examined by the adsorption of benzene and MEK at~ 1000 ppm to reach equilibrium and subsequent heating to 393 K. The adsorbed benzene was totally removed in 0.5 h. However, it took 50 min. for MEK with ~ 2 wt% still remaining on the surface. This suggested that a portion of the MEK is strongly bonded on the surface.

Mangun et al. (1997) have studied the effects of pore size and pore volume on the equilibrium adsorption capacity and the adsorption kinetics for a series of normal alkanes in phenolic based ACFs. For the normal alkane's series, the lower surface area (smaller pore size) materials had higher adsorption capacity for low boiling point gases/vapors and for adsorbing contaminants at low concentration levels. For higher boiling point gases/vapors and for adsorbing contaminants at higher concentration levels, the adsorption capacity was higher for the higher surface area materials (larger pore size) due to larger pore volume.

Chiang et al. (2001) have studied the change of physical–chemical properties of activated carbons by ozonation and its effects on the adsorption of VOCs exemplified by MEK and benzene. The surface physical characteristics analyzed were BET specific surface area, micropore area, micropore volume and pore diameter. The BET surface area of oxidized activated carbon [AC (O_3)] increased by 8.7% over that of the activated carbon (AC). The results indicated that oxidation increased mainly the micropore surface area, which contributed to 74% of the total increase in the specific surface area. Upon oxidation, the micropore volume also increased by 7.5%, along with an insignificant (0.5%) increase in pore diameter. Physical as well as chemical changes were also observed during ozonation. The results indicated that the concentration of oxygen radical within the functional groups, which remains on the surface of the activated carbon, slightly increased by 0.29%, whereas the same for the hydrogen decreased by 0.09% upon ozone treatment. The overall functional groups (–OH, –COOH, -C=O etc.) were increased by 12%. It was concluded that the

adsorption rate by AC(O$_3$) is greater than that by AC, which could be attributed to the change of the physical characteristics of the activated carbon. The MEK adsorption capacity of AC (O$_3$) was greater than that of AC at various MEK concentrations. This was concluded as the surface of AC(O$_3$) is more polar than that of AC and as MEK is a polar adsorbate, the MEK-specific adsorption sites will be more on AC(O$_3$) than AC.

Kang et al. (2002) have studied the breakthrough characteristics of low concentration MEK and benzene vapors in beds packed with rayon-based ACF having different surface areas. A smooth breakthrough curve (sigmoidal) profile was observed for ACFs having relatively larger surface area. However, at lower feedstock concentrations, the concentration of VOCs in the effluent increased gradually with time in the case of ACF having lower surface area, suggesting a large pore diffusion resistance during adsorption. This may be due to the narrow pore entrance in ACF leading to a low adsorption rate. Therefore, the ACF having lower surface area may not possess a good dynamic breakthrough adsorption characteristic, even though it has a higher equilibrium adsorption capacity at low concentrations.

Larson et al. (1995) have developed a new ACC adsorption system that was integrated with electrothermal desorption and cryogenic vapor recovery. A laboratory scale fixed bed reactor was used to adsorb trace amount of VOCs on ACC. Once the adsorption was completed, the ACC was regenerated by electrothermal desorption under a small flow rate of N$_2$ gas. The resulting VOC gas stream was then treated (condensed) cryogenically with liquid nitrogen, making the pure toxic liquid available for reuse

The breakthrough tests were performed on ACC and then with the Calgon BPL activated carbon in packed bed to compare the adsorption dynamics of the two adsorbents. The adsorption capacity results for Calgon BPL and ACC were determined to be 0.307 cm^3/g and 0.553 cm^3/g respectively. The breakthrough time for ACC and Calgon BPL adsorbents were 91.7 min and 47.2 min respectively. It was concluded that ACC have higher adsorption capacity due to higher specific surface area for a higher specific pore volume. Electrothemical desorption was also carried out on ACC, which provided efficient regeneration and faster desorption rates. Stability for in situ electrothermal regeneration, control of pressure drop and easy handling were shown to be the other advantages of ACC in comparison to granular activated carbon (GAC).

Verma et al (2002) have carried out both experimental and theoretical studies on the removal of VOCs by cryogenic condensation and adsorption. The adsorption experiments were mainly designed for the purpose of breakthrough analysis and carried out on both the ACF and activated charcoal under varying operating conditions to determine the relative performance of these materials with that of ACF. It was found that ACF exhibits larger adsorption for VOC than granular activated carbon under identical operating conditions. It was also observed that the breakthrough time during adsorption decreased with the increase in the VOC concentration, whereas condensation rate of VOC decreased with the decrease in the effluent concentration level. Hence, it was concluded, that adsorption was effective if VOCs concentration in the gas were in ppm and sub-ppm levels, whereas cryogenic condensation was found to be effective in relatively higher VOCs concentration levels (>1%). The regeneration of ACF was also carried out by electrical (~ DC 50 V and 15 A) heating. A temperature range of 120-150 ^{0}C and regeneration time 45-60 min were typically required for the complete regeneration of ACF

Subrenat et al. (2001) have carried out the regeneration study on Joule effect in the case of ACC loaded with ethanol. The measurements of electrical resistance according to the intrinsic characteristics of the fabrics and temperature at the surface of the material for various activated carbon cloths have also been done in this study. The regeneration was carried out on ACC loaded with VOCs at a temperature of 100 ^{0}C and 150 ^{0}C and under nitrogen desorption flow velocity of 2.4 m h^{-1}. It was observed from the results that the increase in regeneration temperature to 150 ^{0}C enhances the amount of desorbed compound leading to a desorption yield of 100%. The desorption duration was also short (around 30 min) in comparison with that for lower temperature (100 ^{0}C). The results showed that the electrical resistivity decreased linearly in the studied temperature range. It was also found that the electrical resistivity increased with the specific surface area and the activation with CO_2 results in a higher conductivity of the activated carbon fabrics, compared to steam activation.

Hence, from the literature survey it is evident that quite a few works has been carried out on the equilibrium study to explain the isotherm data, whereas only a limited number of studies have been carried out to determine the breakthrough characteristics of VOCs on ACF under dynamic condition. The focus of the present work is on the application of regenerative type of sorbent, ACF in control of VOCs,

which is also a potential adsorbent for several other gaseous pollutants, such as SO_2, NO_x etc. In this thesis, both experimental and theoretical studies have been carried out to determine the breakthrough characteristics of the ACF during adsorption of VOCs under varying operating conditions. In addition, an electrothermal regeneration has also been studied for the desorption of VOC and making the ACF for reuse. A detailed description of the theoretical analysis and mathematical model, to understand the mechanism of the process is discussed in the next chapter.

CHAPTER 3
THEORETICAL ANALYSIS

In the present chapter, a mathematical model is presented to predict the time-dependent (unsteady state) concentration profiles of the adsorbing species (VOCs) on a solid adsorbent (ACF) under isothermal conditions. One important point that may be noted is that, in reality the steady state conditions never exists in the bed of adsorbing materials during adsorption/desorption. Hence, a finite adsorption/desorption rate always exists in the bed. The steady state is achieved only when the bed reaches saturation levels. The theoretical analysis in this work takes into account the effects of pore diffusion, in addition to the film mass transfer resistance around the fibers on the performance of adsorbents. The principal aspect of the present model is that it is based on non-equilibrium approach and thus incorporates the individual kinetic rate expressions for adsorption and desorption rather than equilibrium or pseudo-stationary assumptions made in most of the models (*Yang, 1997*) developed for adsorption in a fixed bed. By equating the adsorption and desorption rates an appropriate equilibrium isotherm such as *Sips isotherm* is obtained.

The various assumptions made in the theoretical analysis in developing mathematical model for adsorption of VOCs on ACF may be summarized as follows:

(1) Considering the fact that the concentration of VOCs are usually in ppm levels and an unsteady condition exists throughout a typical adsorption/desorption cycle, the effects of exothermic heat on the rate of adsorption were assumed to be negligible (*Verma and Gupta, 2002*).

(2) Negligible pressure drop exists in the bed (*Rood et al. 1995*).

(3) There is a constant fluid velocity throughout the bed.

The present model is based on three governing equations: (a) species balance of the adsorbing component in the bed, (b) species balance of the component inside the pores of the fiber, and (c) surface adsorption within the pores.

Species Balance of the component in the perforated bed:

The experiments were carried out on ACF in cloth form wrapped over a vertical reactor made of Teflon. The outer surface of the reactor was perforated with one end closed. The reactor was encapsulated in a SS tube with provisions for gas inlet and

outlet. The VOC laden gas fed to the reactor came out radially into the SS tube. Consider a gas flow in a perforated bed of ACF under isothermal condition, in which pressure drop is negligible and there is no variation in fluid velocity in the radial direction the bed. By making a species balance in the gaseous phase in the ACF bed of porosity,ε, the equation is obtained as follows:

$$\frac{\partial C_a}{\partial t} + V_R \frac{\partial C_a}{\partial R} - \frac{D_R}{R}\frac{\partial}{\partial R}(R\frac{\partial C_a}{\partial R}) + (\frac{1-\varepsilon}{\varepsilon})k_m a(C_a - C_F^s) = 0 \qquad (3.1)$$

The terms on the left hand side of Eq. (3.1) are transient, convection (radial direction), dispersion and mass transfer rate from the bulk gas to the fiber surface, respectively

Here,

C_G = Interfiber concentration of the species, at any arbitrary location r in the bed.

V_R = Gas velocity in the radial direction

D_R = Radial dispersion coefficient in the perforated bed

a = external surface area per unit volume of the fiber

= 4.0/ D_f

D_f = Diameter of the fiber

k_m =   average mass film transfer coefficient around the fiber.

C^S_F = Concentration at the outer surface of the fiber

Mass Balance of the component inside the pores of the fiber:

Assuming the shape of the pores to be spherical, the concentration of the species, C_p in the pore is obtained from the following equation:

$$\alpha\frac{\partial C_p}{\partial t} + \frac{i}{r^2}\frac{\partial}{\partial r}\left(r^2 N_r\right) + a^{\oplus}\frac{\partial C_s}{\partial t} = 0 \qquad (3.2)$$

In the above equation the terms in the left hand side are transient, diffusion and adsorption terms, respectively.

Here,

C_p = Molar concentration of species at a location r inside the pores

α = Intrafiber void fraction

$a^{\oplus}$ = Total adsorption surface area per unit volume of the fiber

N_r = Molar diffusion flux of the component in the radial direction

C_s = Molar surface concentration of adsorbed species inside the pores

Adsorption/desorption within the pores:

The rate of change of surface concentration of the adsorbed species $\dfrac{\partial C_s}{\partial t}$ is determined from the individual surface rates of adsorption and desorption

$$\frac{\partial C_s}{\partial t} = k_a C_p \left[1 - \left(\frac{C_s}{C_{s\,max}} \right) \right]^N - k_d \left(\frac{C_s}{C_{s\,max}} \right)^N \qquad (3.3)$$

Here, k_a and k_d are adsorption and desorption rate coefficients.

At equilibrium, as the change in the surface concentration is zero, i.e. $\dfrac{\partial C_s}{\partial t} = 0$, the corresponding isotherm for C_s can be obtained from equation (3.3) by equating the adsorption and desorption rates as follows.

$$C_s = C_{s\,max} \left[\frac{(KC_p)^{1/N}}{1 + (KC_p)^{1/N}} \right] \qquad (3.4)$$

Here K = adsorption equilibrium constant = $\dfrac{k_a}{k_d}$

The above equation is known as the *Sips isotherm* (*Do et al, 1998*) for single component system. As shown in equation (3.4), the Sips isotherm has three parameters; C_{smax}, K, and N, which are usually obtained from the experimental adsorption data under equilibrium condition. It may be pointed out that alternate kinetic rate expressions obtained from other isotherms including the extended Langmuir and Temkin can also be used to determine the rate of change of surface concentrations. In the present study, the Sips isotherm was selected due to the fact that the Sips isotherm has been found to explain the equilibrium isotherm data for a number of VOCs e.g. benzene, toluene and xylene etc (*Do et al, 1998*).

The governing equations (3.1-3.3) are the basis of the model developed in this study for predicting the adsorbents performance in the bed. These equations are coupled partial differential equations, with time (t) and radial directions (both R and r) as independent variables. Hence, in the present work an approach is adopted to simplify the numerical computations and reduce the CPU time. In this approach radial concentration profiles within the pores are averaged and the average surface and gas phase concentrations within the pores of the fiber are determined (*Yang, 1997; Verma, 2002*). The detailed computational steps are shown below:

First, the particle volume average quantities (Yang, 1997) are calculated as follows:

$$\overline{C_p} = \frac{3}{R_f^3} \int_0^{R_f} C_p r^2 dr \tag{3.5}$$

$$\overline{C_s} = \frac{3}{R_f^3} \int_0^{R_f} C_s r^2 dr \tag{3.6}$$

Where $\overline{C_p}$ and $\overline{C_s}$ are the volume average surface concentrations in the pores and on the surface, respectively and R_f is the radius of the fiber.

Second, by integrating equation (3.2) with respect to r and using volume averaged quantities and noting that $N_R = 0$ at r=0 (due to symmetricity), the following equation is obtained:

$$\alpha \frac{\partial \overline{C_p}}{\partial t} + \frac{3}{R_f} N_R^s + a^\oplus \frac{\partial \overline{C_s}}{\partial t} = 0 \tag{3.7}$$

Where, N_R^s is the diffusional flux at the fiber surface.

At the fiber surface, the diffusing flux into or out of the pores, N^s is given by

$$N_R^s = -k_m (C_G - C_F^s) \tag{3.8}$$

Finally, to further simplify the model, a parabolic concentration profile within the pores of the fiber is assumed, which is a good assumption when compared with the profiles obtained from rigorous approach (Yang, 1997). Thus we have the following assumed expression for C_p.

$$C_p = E + Fr^2 \tag{3.9}$$

Where the constant E and F can be evaluated by using surface condition:

$$C_p = C_F^s, \ at \ r = R_f$$

$$E = C_F^s - FR_f^2$$

By integrating equation (3.9) and again using the volume averaged quantities, F is computed as follows,

$$F = (C_F^s - \overline{C_p}) \frac{5}{2R_f^2} \tag{3.10}$$

C_F^s is determined by equating mass flux across the external gas film to that at the mouth of the pores within the fibers:

$$K_m(C_G - C_F^s) = D_e\left(\frac{\partial C_p}{\partial r}\right)_{r=R_f} = 2D_e FR_f \tag{3.11}$$

From the above expression C_F^s is obtained in terms of independent variables C_p and C_G is as follows,

$$C_F^s = \frac{k_m C_G + 10(D_e/D_f)\overline{C_p}}{(k_m + 10D_e/D_f)} \tag{3.12}$$

Here, D_e is effective diffusivity inside the pores

Hence, by the approximation mentioned above equation (3.7) can be rewritten as:

$$\frac{\partial \overline{C_p}}{\partial t} - \frac{3}{R_f \alpha}k_m(C_G - C_f^s) + \frac{a^\oplus}{\alpha}\frac{\partial \overline{C_s}}{\partial t} = 0 \tag{3.13}$$

In the present model, the simplified governing equations (3.1), (3.3) and (3.13) completely describe adsorption/desorption behavior of a single component VOC (toluene) in a perforated bed of ACF in a gas flow under isothermal condition.

Initial and boundary conditions for the above equations are as follows:

At t=0, $\quad C_G = C_{Gi} \quad \overline{C_s} = C_{s\max}\left[\frac{(KC_{Gi})^{1/N}}{1+(KC_{Gi})^{1/N}}\right], \quad \overline{C_p} = C_{Gi}$ \hfill (3.14a-c)

where, C_{Gi} is the concentration of trace amount of VOC which may be present in the bed.

At $R = R_1$, $\quad C_G = C_{Gf}, \quad \overline{C_s} = C_{s\max}\left[\frac{(KC_{Gf})^{1/N}}{1+(KC_{Gf})^{1/N}}\right], \quad \overline{C_p} = C_{Gf}$ \hfill (3.15a-c)

where, C_{Gf} is the concentration of VOC in the feed stream

At $R = R_2$, $\quad \dfrac{\partial C_G}{\partial r} = 0, \quad \dfrac{\partial \overline{C_p}}{\partial r} = 0, \quad \dfrac{\partial \overline{C_s}}{\partial r} = 0$ \hfill (3.16a-c)

Non-dimensionalisation of governing equations and initial and boundary conditions:

The following dimensional variables are introduced to render the governing equation dimensionless:

Bulk Gas Concentration

$$C_G^* = \frac{C_G}{C_{Gf}}$$

Average gas concentration inside the pore

$$\overline{C_P}^* = \frac{\overline{C_P}}{C'_{if}}$$

Average Adsorbed Phase concentration

$$\overline{C_s}^* = \frac{\overline{C_s}}{C'_{s\,max}}$$

Time

$$t^* = \frac{t}{\tau}, \quad \tau = \frac{L_{bed}}{V}$$

Distance in radial direction

$$\xi = \frac{R - R_1}{R - R_2}$$

Introducing the dimensionless variables $(C_G^*, \overline{C_P}^*, \overline{C_s}^*, \ t^*$ and $\xi)$ in governing equations (3.1), (3.3) and (3.1.3) the following three non-dimensionalised equations are obtained:

$$\left(\frac{\xi + A}{C\xi}\right)\frac{\partial C_G^*}{\partial t^*} + \frac{B}{C\xi}\frac{\partial C_G^*}{\partial \xi} + \frac{D}{C\xi}(\xi + A)(C_G^* - C_F^{s*}) = \frac{1}{\xi}\frac{\partial}{\partial \xi}\left[\xi\left(1 + \frac{A}{\xi}\right)\frac{\partial C_G^*}{\partial \xi}\right] \quad (3.17)$$

Here, $A = \left(\dfrac{R_1}{R_2 - R_1}\right)$; R_1 and R_2 are the inner and outer radius of the bed respectively.

$B = \left(\dfrac{Q}{2\pi V}\right)\dfrac{1}{(R_2 - R_1)^2}$; Q and V are the volumetric flow rate and the superficial velocity of the gas respectively.

$C = \dfrac{D_R}{(R_2 - R_1)^2}\left(\dfrac{L_{bed}}{V}\right)$; Lbed is the length of the bed

$$D = \left(\frac{1 - \varepsilon}{\varepsilon}\right)k_m a\left(\frac{L_{bed}}{V}\right)$$

$$\frac{\partial \overline{C}_p^{*}}{\partial t^{*}} - E(C_G^{*} - C_F^{s*}) + F\frac{\partial \overline{C}_s^{*}}{\partial t^{*}} = 0 \tag{3.18}$$

here, $E = \dfrac{3}{R_f}\left(\dfrac{k_m}{\alpha}\right)\left(\dfrac{L_{bed}}{V}\right)$; R_f is the radius of the fiber

$$F = \frac{a^{0}}{\alpha}\frac{C_{s\,max}}{C_{Gf}}$$

$$\frac{\partial \overline{C}_s^{*}}{\partial t^{*}} = G\overline{C}_p^{*}(1 - \overline{C}_s^{*})^{N} - H(\overline{C}_s^{*})^{N} \tag{3.19}$$

here, $G = \dfrac{k_a C_{Gf} L_{bed}}{C_{s\,max}V}$ and $H = \dfrac{k_d L_{bed}}{C_{s\,max}V}$

Here A, B, C, D, E, F, G and H are intermediate coefficients of the governing equations.

C_F^{s*} In Eq. (3.18) can also be written as follows,

$$C_F^{s*} = \frac{C_F^{s}}{C_{Gf}} = \frac{\left(C_G^{*}k_m + \dfrac{10D_e}{D_f}\overline{C}_p\right)}{\left(k_m + \dfrac{10D_e}{D_f}\right)} \tag{3.20}$$

The dimensionless initial and boundary conditions can be rewritten as follows,

at $t^{*} = 0$, $C_G^{*} = \dfrac{C_{Gi}}{C_{Gf}}$, $\overline{C}_s^{*} = \left[\dfrac{(KC_{Gi})^{1/N}}{1 + (KC_{Gi})^{1/N}}\right]$, $\overline{C}_p^{*} = \dfrac{C_{Gi}}{C_{Gf}}$ (3.21a-c)

at $\xi = 0$, $C_G^{*} = 1$, $\overline{C}_s^{*} = \left[\dfrac{(KC_{Gf})^{1/N}}{1 + (KC_{Gf})^{1/N}}\right]$, $\overline{C}_p^{*} = 1$ (3.22a-c)

at $\xi = 1$. $\dfrac{\partial C_G^{*}}{\partial \xi} = 0$, $\dfrac{\partial \overline{C}_p^{*}}{\partial \xi} = 0$, $\dfrac{\partial \overline{C}_s^{*}}{\partial \xi} = 0$ (3.23a-c)

Numerical solution technique

For a system of one adsorbing component in an inert gas, we have three

18

partial differential equations (3.1), (3.3), (3.13) containing three dependent variables C_G, $\overline{C}_p$, $\overline{C}_s$, which are function of time and radial location. These equations are solved simultaneously by finite difference method using a Fortran subroutine D03pcf of NAG Fortran library. The Fortran codes are given in the appendix.

CHAPTER 4
EXPERIMENTAL STUDIES

In this section details of the experimental set-up used to study adsorption/desorption characteristics of VOCs on ACF are described. The experiments were carried on two different types of ACF samples having different BET surface area (one procured locally and the other imported) under several operating conditions, such as bed temperature, inlet concentration of VOCs, gas flow rate and weight of ACF. Both of the above mentioned ACF samples are obtained from viscous rayon precursor.

4.1 Experimental Set up:

Figure 4.1 is the schematic diagram of the experimental set-up used in this study. The experimental set up may be assumed to consist of three sections as shown in Figure 4.1: (a) gas preparation section, (b) test and (c) analysis sections. In the gas preparation section, nitrogen gas was bubbled in a vertical bottle containing the VOC liquid at a constant temperature to prepare the gas of desired VOC concentration. The bubbler used to bubble the gas was a SS made tube whose bottom end was closed and the outer surface were perforated up to a distance of 10 cm from the bottom end, with perforated holes of diameter 0.08 mm. The entire perforated section of the bubbler was submerged in the VOC liquid. The level of the liquid in the bottle was maintained high enough to provide sufficient residence time to the carrier gas for complete saturation with VOC. The bottle was kept inside the Freon (R-11) refrigeration unit. Therefore, by controlling the temperature the vapor pressure of VOCs and hence, the required partial pressure were achieved. Hence, this way the required VOC concentration was maintained. The required flow rates of nitrogen over a range of *0.2-1.0 slpm* were controlled and monitored by mass flow controller (Bronkhorst, Netherlands). Prior to bubbling the carrier gas (nitrogen in this case) through the VOC liquid, it was passed through two consecutive gas purification sections. The first purification section containing silica gel was used to remove moisture and the second one containing molecular sieves was used to remove trace amount of hydrocarbons which may be present in the carrier gas. The test section consisted of a vertical Teflon made reactor (*I.D = 2.5 cm, O.D = 2.8 cm, L = 10 cm*) encapsulated in a SS shell (*I.D = 4.0 cm, L = 20 cm*) with provisions for gas inlet and outlet. Inside the SS shell the teflon reactor was vertically and co-axially mounted, with one end closed. The outer

surface of the reactor was perforated with the holes of diameter *0.1 mm* and center to center distance of *0.5 cm*. The experiments were carried out on ACF in cloth form wrapped over the reactor. Thermocouple used to monitor the bed temperature was mounted vertically at the center of the reactor. There was a provision for varying the bed temperature from 35 to 100^0 C with the aid of electrical heating and PID controller (FUJI Electric, Japan). The effluent gas stream from the reactor was passed to the analytical section. The analytical section consisted of gas chromatography (GC) with FID and data station. A computer was connected to the data station to store the chromatograph and the peak areas.

4.2 Experimental Procedure

The required amount of ACF sample *(~5 g)* was weighed by electronic balance and then pretreated before carrying out the test runs. The pretreatment was carried out at a temperature of ~150 °C and under vacuum for 4 hours. This combination of temperature and vacuum pressure were obtained after a series of test runs for the optimum performance of ACF. The ACF sample was then wrapped over the Teflon reactor. Prior to start of the experiment, the bottle was filled with *140 ml* of VOC and kept inside the refrigeration unit. For a particular VOC inlet concentration, the corresponding saturation temperature of the refrigeration unit and hence the VOC bottle temperature was set. Then the refrigeration unit was allowed sufficient time *(~1.5 hrs.)* to attain the required temperature. The reactor was heated to the desired bed temperature *(~50 ^{0}C)* and further kept at that temperature for 1 hr so that the system was stabilized and a uniform temperature existed in the bed. The required flow rate of the gas was controlled using MFC. The concentration of the inlet gaseous mixture in the line bypassing the reactor was measured by GC prior to the start of the adsorption process. As the adsorption was started, the concentration of exit gas from the reactor was monitored and measured by GC.

4.3 Product Analysis

The product gas was analyzed by GC using Porapak and Chromosorb columns *(length 15 mm, I.D = 2.0 mm)*. The first one was used as a reference column and the later one was used to separate nitrogen and toluene gas. Flame ionization detector (FID) was used to detect the components at different retention times. The temperature of the injector, detector, oven and oven final were maintained constant at 170 ^{0}C, 180

^{0}C, 140 ^{0}C and 150 ^{0}C, respectively. Nitrogen was used as a carrier gas with a flow rate of 27 ml/min and a pressure of 3.8 kg/cm^2. All the GC data were stored in a computer using a data station (Winchrom software) connected between the chromatograph and the computer. The areas obtained in a computer were in proportion to the concentrations as pre-defined in the software.

4.4 Experimental variables:

The experiments were performed in a fixed bed reactor under different operating conditions shown in Table 4.1. Most of the possible combinations of bed temperature, inlet VOC concentration, gas flow rate, amount of ACF were selected for study.

Experimental Conditions				
Inlet VOC Concentration (ppm)	2000	4000	6000	10000
Gas flow rate (slpm)	0.2		0.5	1.0
Bed temperature (^{0}C)	35	40	50	75	100
Sorbents amount (gm)	2.2		4.5	8.5
BET areas (m^2/g)	1000 (procured locally)		1700 (imported)	

Table 4.1: Different experimental variables for VOC adsorption

The experiments were carried out at various VOC inlet concentrations ranging from 2000 to 10000 *ppm*, whereas the gas flow rates ranged between 0.2 to 1.0 *slpm*. A few

numbers of experiments were also carried out at six different bed temperatures in the range of 35 to 100 °C to study the effect of bed temperature. Effects of weight of ACF on the adsorption of VOCs were also studied for various amount of ACF taken. Here, 2.2 g of ACF corresponds to 1 wrap, whereas 4.5 and 8.5 corresponds to 2 and 3 wraps respectively.

4.5 Regeneration of ACF:

The schematic diagram for the regeneration (or desorption) of ACF is shown in Figure 4.2. The regenerations were carried out to make the ACF available for subsequent use. The regenerations of ACF were carried out by electrical (~ DC 20 V and 3 A) heating under a low nitrogen flow rate of 0.2 slpm. A temperature of ~150 ^{0}C and regeneration time of 60-75 min were typically required for the complete regeneration of ACF. The temperature was monitored by a thermocouple fixed at the surface of the ACF sample. The voltage and current were measured by voltmeter and ammeter, respectively. The concentration of the exit gas from the reactor was measured with the help of GC using FID.
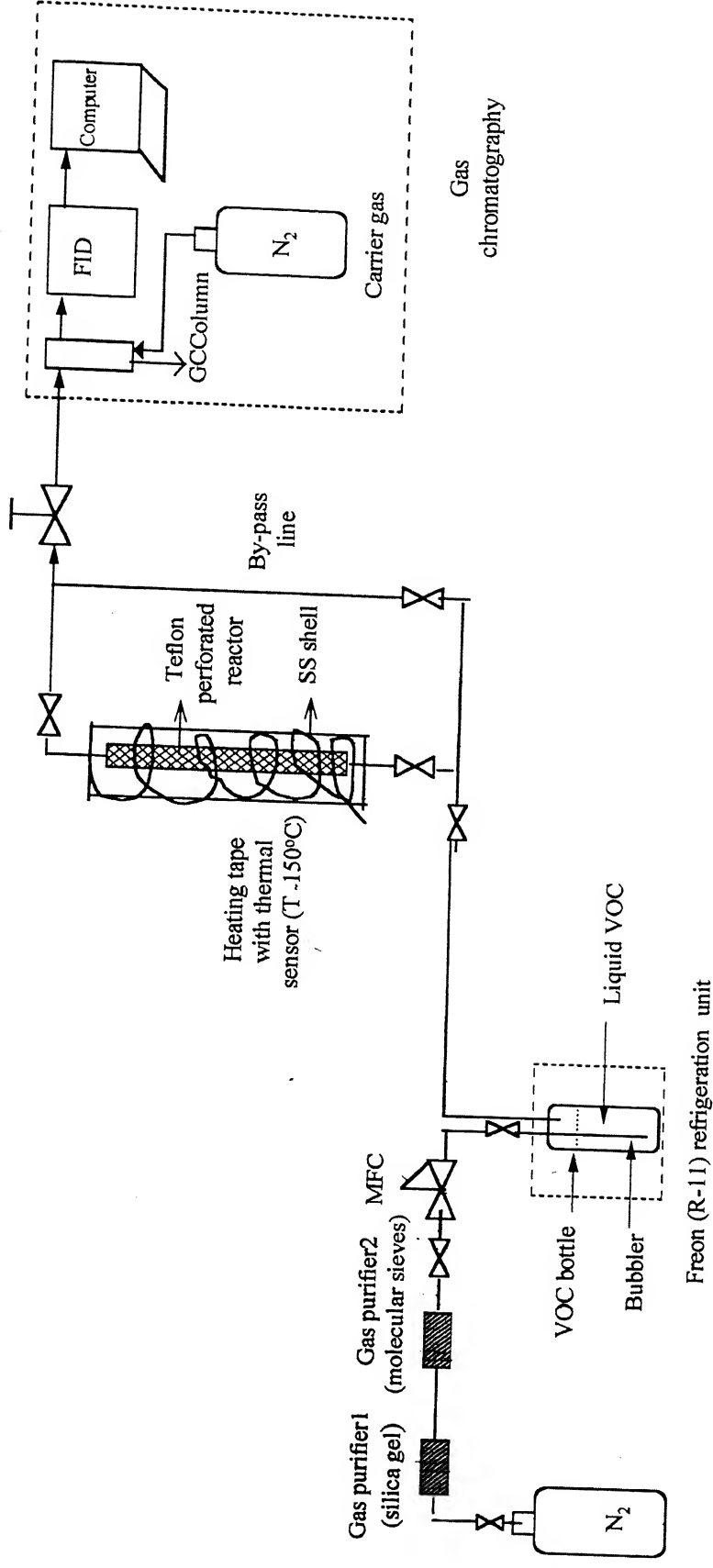
Fig 4.1: Schematic diagram of experimental set-up for VOC adsorption/desorption study on ACF

Fig. 4.2: Schematic diagram for the regeneration of ACF

25

CHAPTER 5
RESULTS AND DISCUSSION

This chapter describes the experimental and model predicted results obtained for the removal of VOC by adsorption on ACF under varying operating conditions, such as inlet concentration of VOC, bed temperature, flow rate of the gas and weight of ACF. The results have been analyzed from breakthrough point of view. The experimental results are compared and explained, wherever possible, with the model simulated result.
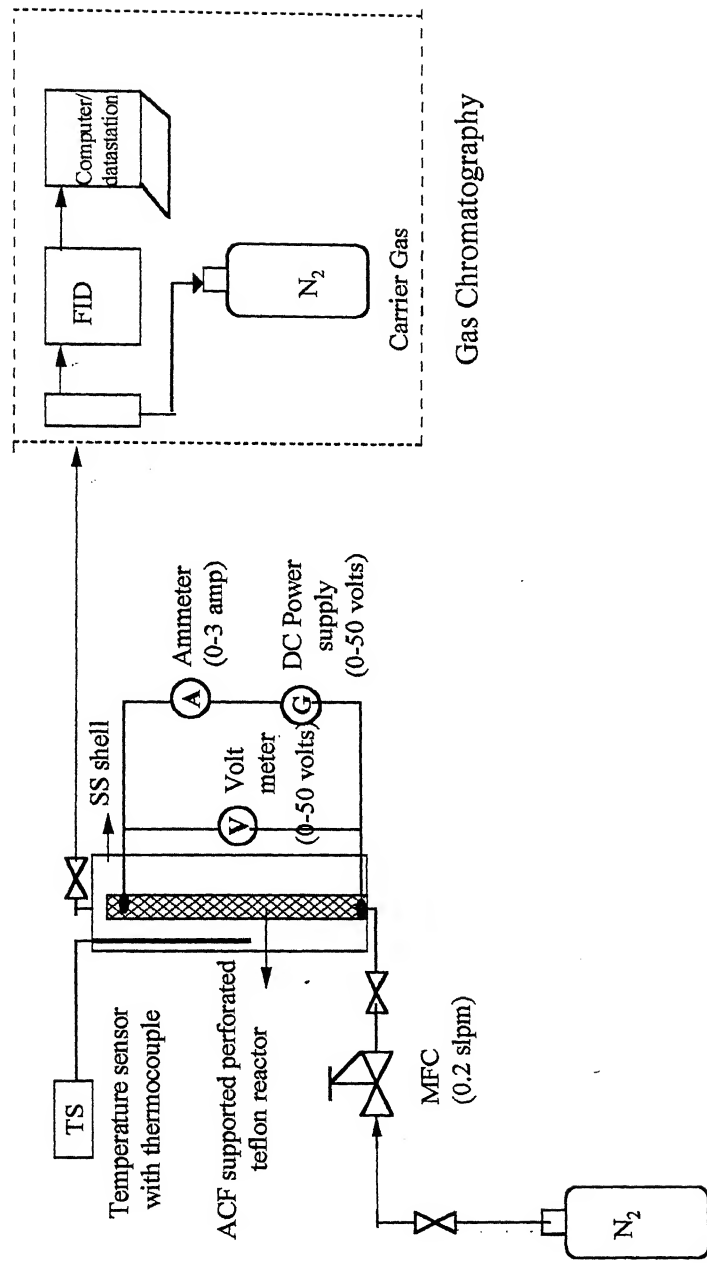
The term *breakthrough* refers to the response of an initially clean bed (*i.e.* free of adsorbate) to an influent containing an adsorbate or a mixture of adsorbates and a *breakthrough curve* is the history of the effluent concentration from a bed subject to a stepped concentration in input. The shape of a breakthrough curve is determined by the nature or type of the adsorption isotherm. In addition, it is influenced by the individual transport processes in the bed and within the particles or fibers (macro or micropores). In the typical experiments performed to study the effects of several operating conditions, the teflon made reactor bed wrapped with fresh ACF was heated to a certain bed temperature and fed with a gas containing the calibrated mixture of nitrogen and toluene at a constant flow rate. During the initial stage of adsorption process, most of the VOC entering the bed is removed by adsorption occurring at the surface of the pores. During this stage of adsorption, no or very low concentration of VOC is observed at the reactor outlet. However, as the adsorption proceeds with time, the adsorption sites of the ACF are occupied by the VOC molecules making them unavailable for further adsorption. This phenomenon (saturation of ACF bed) initially takes place at the entrance region of the reactor and gradually proceeds towards the exit. Thus, in the saturated bed region there is an elutriation and mass transfer is confined within a small region (zone). This process continues till the overall adsorption process is completed and entire bed is saturated with VOC. Under this condition, the VOC concentration at the reactor outlet becomes equal to that at the inlet. In the present study, the change in VOC concentration with time at the reactor outlet was determined using gas chromatography. Such transient behavior of concentration is called breakthrough and the corresponding concentration vs. time plot is called breakthrough curve.

Various quantities required in the model analysis such as, superficial gas velocity, bed porosity, density of the gas, Reynolds number, Schmidt number, dispersion coefficient, Peclet number and mass transfer coefficient, were calculated under the experimental conditions. These calculations have been presented in the appendix.

5.1 Effect of bed Temperature on adsorbent

To determine the effects of bed temperature on the VOC removal, the experiments were carried out at varying bed temperatures (35, 40, 50, 75 and 100 ^0C). The inlet concentration of VOC (toluene) was kept constant at 10000 ppm (the corresponding cooling bath temperature to obtain the desired vapor pressure of VOC and hence, the required partial pressure in the gaseous mixture was kept constant at - 1.69 ^0C). In all the runs, the experiments were carried out on 5 g of the ACF sample and at a constant gas flow rate of 0.5 slpm. Figure 5.1 describes the experimentally obtained breakthrough characteristics of VOC during dynamic adsorption by ACF (Type-1 sample) carried out at five different temperatures. It may be observed from Figure 5.1 that the breakthrough times are approximately 7 min for both the temperatures: 35 and 40 ^{0}C. However, the total adsorption time (time for the exit gas concentration to approximately reach the inlet concentration, 10000 ppm) is slightly greater at 40 ^{0}C (40 min) than at 35 ^{0}C (30 min). However, both the breakthrough and adsorption times were found to increase to 10 and 50 min, respectively at the bed temperature of 50 ^{0}C. Further increase in bed temperature to 75 ^{0}C resulted in significance decrease in both breakthrough time (6 min) and total adsorption time (30 min). As also observed from the figure, the breakthrough curve further shifted to the left as the bed temperature was increased to 100 ^{0}C, indicating an early saturation of the bed. The similar experiments were carried out on ACF (Type-2 sample), under the identical operating conditions to study the effect of bed temperature on the VOC adsorption process. The breakthrough curves for the adsorption of VOC on the ACF (Type-2 sample) under various temperatures are described in Figure 5.2. It may be observed from Figure 5.2 that there was practically no improvement in the breakthrough time with an increase in the bed temperature from 35 to 50 ^{0}C. In each case the breakthrough occurred in approximately 20 min. However the total adsorption times were 50, 60 and 70 min for the bed temperatures of 35, 40 and 50 ^{0}C respectively. Here also, further increase in bed temperature to 75 ^{0}C resulted in

decrease in both the breakthrough time (12 min) and the total adsorption time (42 min). It is also observed from Figure 5.2 that the breakthrough curve shifted sharply to the left as the bed temperature was increased to 100 ^{0}C. Thus, from these results it was concluded that a bed temperature of 50 ^{0}C is most favorable for capturing toluene vapor from the effluent and therefore, henceforth all the remaining experiments in this study were carried out at 50^{0}C. The breakthrough and total adsorption times for two types of ACFs at different bed temperatures are summarized in Table 5.1. The difference in the performance of the two types of ACF samples in capturing VOC due to the difference in BET surface area and pore size are discussed later in section 5.6.

The model predictions were done under identical operating conditions to explain the breakthrough of VOC in the ACF bed. The VOC adsorption by ACF in a fixed bed under isothermal condition is considered to be controlled by three rate mechanism as discussed in the theoretical section,

(a) diffusion of the species from bulk gas to the fiber surface through a gas film surrounding the fiber (bulk diffusion).

(b) diffusion of the gas within the pores (pore diffusion)

(c) adsorption /desorption of VOCs inside the pores (surface reaction).

The diffusion of the gas from the bulk to the fiber is dependent on mass transfer coefficient, which in turn is determined by the diameter of the fiber and gas flow rate. The mass transfer coefficient is shown to be dependent on Sherwood number which in turn, is a function of the particles Reynolds number and Schmidt number. Under the existing experimental conditions (over a temperature range of 30 to 50 ^{0}C) the Reynolds number was calculated to be constant at $4.142 \, x \, 10^{-5}$, since in all the cases the gas flow rate and the diameter of the fiber were kept constant, whereas Schmidt number was found to marginally vary (5%) in the range of 1.38 to 1.45. Hence, in each case the effect of bulk diffusion was the same. The diffusion of the gas in the pores is primarily dependent on the pore size of the sorbents. With increase in the temperature the pore diffusion coefficient is expected to be higher and favorable for pore diffusion. However, over a temperature range of 35 to 50 ^{0}C a marginal increase in pore diffusion from $1.118 \, x \, 10^{-7}$ to $1.145 \, x \, 10^{-7}$ m^2/s was observed. The main reason for longer breakthrough time at higher temperature was attributed to a higher rate constant because of its Arrhenius type of temperature dependence.

If we recall Equations (3.3-3.4) derived in the chapter on theoretical analysis, the Sips isotherm equation was obtained by equating the adsorption and desorption rates

under equilibrium condition. Therefore, the Sips isotherm parameters b and $C_{s\mu}$ have been used wherever necessary as adjustable parameters in the present model to explain the experimental data. The numerical values of these parameters for the propane-activated carbon system have been reported by Do (1998). For the present work (toluene-ACF system) these numbers were used as a guideline for explaining the breakthrough characteristics of VOC by model prediction. Figures (5.3-5.4) compare the model predicted breakthrough curves with the experimental data for the Type-1 and Type-2 ACF samples, respectively. A reasonable good agreement is observed between the two results within the experimental and computational errors. In each case the data could be explained by the model with a marginal change in the model parameters, b (from 10.0 to 8.5) and $C_{s\mu}$ (from 0.75 to 0.95) over a temperature range of 35 to 50 ^{0}C. The temperature dependency of the Sips isotherm parameters are as follows (Do, 1998):

$$b = b_\infty \exp\left[\frac{Q}{R_g T}\right] \quad \text{and} \quad C_{\mu s} = C_{\mu s,0} \exp\left[\chi\left(1 - \frac{T}{T_0}\right)\right]$$

Here, b_∞ is the adsorption affinity constant at infinite temperature and $C_{\mu s,o}$ is the saturation capacity at the reference temperature T_0. Hence, from the above equations it is clear that, with the increase in temperature b will decrease, whereas there will be an increase in the values of the parameter $C_{\mu s}$ as obtained in the present study. The adsorption equilibrium constants K, is defined as the ratio of adsorption rate constant (k_a) to desorption rate constant (k_d). The values of k_a can be calculated by using the formula which is obtained from kinetic theory of gases. Once the value of k_a is obtained, the k_d can be calculated by using the formula incorporating k_a and which is obtained by proper mathematical derivation. The values of K were determined to be 25.60, 23.94 and 22.82 m^3/mol for Type1 ACF at 35, 40, and 50 ^{0}C, respectively and 21.76, 20.95 and 20.14 m^3/mol, respectively for Type-2 ACF under the identical temperatures. The numerical values of K for two types of samples under various temperatures are reported in Table 5.2. The exothermic heats of adsorption were calculated by using the vant Hoff equation:

$$\ln\frac{K_2}{K_1} = \frac{-\Delta H}{R}\left[\frac{1}{T_2} - \frac{1}{T_1}\right]$$

Under the existing experimental conditions the heats of adsorptions determined from the slope of lnK vs 1/T curve were found to be 1.45 and 1.01 kc/mol for Type-1 and

Type-2 ACF, respectively, as shown in the inset of Figures 5.3 and 5.4. The adjusted parameters of Sips isotherm for toluene are reported in Table 5.3 (for Type1 ACF) and Table 5.4 (for Type 2 ACF).

5.2 Effect of concentration:

To determine the effects of VOC concentration at trace levels on the breakthrough characteristics, the experiments were carried out for varying VOC inlet concentrations: 2000, 4000, 6000, and 10000 ppm. For each run 5 gm of the ACF sample was taken. The bed temperature was kept constant at 50 ^{0}C and the flow rate at 0.5 slpm. Figures (5.5-5.6) describe the experimentally obtained toluene breakthrough curves under various inlet concentrations for Type-1 and Type-2 ACF samples, respectively. As observed from Figure 5.5, the breakthrough times are less than 10 min in each case for Type-1 sample, whereas the total adsorption time decreases from 70 to 40 min as the inlet concentration is increased from 2000 to 10000 ppm. For Type-2 sample, referring Figure 5.6, the breakthrough times are observed to be approximately 10 min in each case. However, the total adsorption time decreases from 80 to 50 min as the concentration level is increased from 2000 to 10000 ppm. The breakthrough and the total adsorption times are listed in Table 5.5 for both types of ACF samples. As also observed from these results, decrease in total adsorption time with the increase in concentration is relatively larger at higher concentration levels (4000-10000) than lower concentration levels (2000-4000) in case of both types of the samples, indicating suitability of ACF in capturing toluene vapor at the concentration levels less than 1% (10000 ppm). The increase in the breakthrough and total adsorption times with the decrease in inlet concentration levels as observed from Figures (5.5-5.6) can be explained in terms of the total amount of VOC. With decrease in the inlet concentration under identical flow rates, the total amount of VOC (moles) entering the micro-pores of the fiber is less. Therefore, the saturation of the ACF bed is delayed and occurs in relatively longer time.

Figures (5.5-5.6) show that the model predictions agree well with the experimental results. For the model predictions of the breakthrough curves under identical experimental conditions, variations in the model parameters b and $C_{s\mu}$ were required over the inlet concentration range of 2000 to 10000 ppm. In the case of Type-1 sample b was varied from 23 to 8.5 (kPa)$^{-1}$, while $C_{s\mu}$ was varied from 0.38 to 0.95 (mmol/g). Similarly, in the case of type-2 sample b was varied from 45 to 7.5

$(kPa)^{-1}$ and $C_{s\mu}$ from 0.49 to 1.70 (mmol/g) for an inlet concentration of 2000 and 10000 ppm, respectively. In each case, a substantial variation in the calculated values of the adsorption equilibrium constant was observed. The value of K in the case of Type-1 sample was found to increase from 25.6 to 61.79 m^3/mol corresponding to a concentration change from 10000 to 2000 ppm. On the other hand, for Type-2 sample these values were found to be 20.16 and 120.8 m^3/mol under the identical concentration levels. The slopes of K vs concentration plots as depicted in the respective insets of Figures (5.5-5.6) indicate a nonlinear type of adsorption isotherm over the selected concentration range. This is consistent with the Sips isotherm assumed in this study for adsorption of toluene on ACF surface. The values of K at various concentration levels for both types of ACF samples are reported in Table 5.6. As observed from Table 5.6 the adsorption equilibrium constant K in the case of Type-2 sample is consistently greater than that in the case of type-1 sample over the entire concentration range. Hence, from these results it can be concluded that, the adsorption capacity of Type-2 sample is greater than that for Type-1 sample under identical concentration levels. The superior performance of the Type-2 sample over the Type-1 sample in capturing VOC may be attributed to the difference in BET surface area and pore size, which would be discussed later in section 5.6.

5.3 Effect of flow rate:

To observe the effect of flow rate on the VOC removal, the experiments were carried out at different gas flow rates: 0.25, 0.5 and 1.0 slpm. In each case the bed temperature was fixed at the optimum reaction temperature of 50 ^{0}C. The weight of the sample and the inlet gas concentration were kept constant at 5 gm and 10000 ppm, respectively. Figure 5.7 describes the experimentally obtained VOC breakthrough curves under the above mentioned flow rates. As observed from Figure 5.7, the breakthrough time decreases from 20 to 3 min as the flow rate increases from 0.25 to 1 slpm. The corresponding times to reach 10000 ppm were 55 and 14 minutes, respectively. The breakthrough time and the total adsorption time for all the flow rates are listed in Table 5.7.

Figure 5.7 also compares the experimental data with the model predictions. Good agreements are observed between the two results within the experimental and computational errors. However, at lower flow rate an overshoot is observed in the model predicted breakthrough curve, which is attributed due to the computational

error involved in the numerical scheme adopted in this work. A finite difference method as per the NAG Fortarn subroutine D03pcf was used to solve the partial differential equations. In principle, values of the model parameters b and $C_{s\mu}$ should not vary with the variation in the flow rates. Expectedly, as observed from Table 6 the values of the adjustable parameters b and $C_{s\mu}$ were kept constant at 8.5 kPa^{-1} and 0.95 mmol/g, respectively for each case. Further experiments were carried out at the identical flow rate to determine the repeatability in the data. Figure 5.8 reveals a reasonably good repeatability between the data obtained under two sets of experiments.

As also observed from Figure 5.7, both the breakthrough time and the total adsorption time decreased with increase in flow rate. This can be explained in terms of the particle mass transfer coefficient, k_m. The diffusion of the gas from the bulk to the fiber surface is dependent on k_m, which in turn is a function of Sherwood number, Sh, where, $Sh = \dfrac{k_m D_p}{D_m}$ and D_m and D_p are the molecular diffusivity and particle diameter, respectively. Sherwood number was calculated from the following correlation: $Sh = 2.0 + 1.1(Sc)^{0.33}(Re)^{0.6}$ (Yang, 1999)

Here, Re, Reynolds number is dependent on the diameter of the fiber and gas superficial velocity. It may be pointed out that in the absence of any correlation reported in the open literature for the dispersion coefficient in a radial flow as prevalent in the present situation, the above correlation available for determining the axial dispersion coefficient in a fixed bed filled with the adsorbent materials was used to determine the radial dispersion coefficient over a very small thickness (0.13 cm) of the fabric material (ACF). The effects of dispersion coefficients on the breakthrough curve will be discussed later in the section on the model parametric study.

The diameter of the ACF sample used was very small (4.6 x 10^{-7} m in this case). Similarly, the gas velocity in the existing experimental conditions was also small in the range between 4.5 x 10^{-5} and 2.47 x 10^{-3} m/s, corresponding to flow rates of 0.25 slpm and 1.0 slpm, respectively. Hence, due to small fiber size and small gas flow rate, the Reynolds numbers were calculated to be very small (almost constant at 4.14 x 10^{-5}). Therefore, it is evident from the above correlation, the Sherwood number became independent of superficial gas velocity (Re) resulting in a constant mass transfer coefficient and dependent only on molecular diffusivity and fiber

diameter. The fiber diameter being very small, the mass transfer coefficient was calculated to be very large at 41.24 m/s. The numerical values of various parameters used in this model such as superficial velocity, Reynolds number, Sherwood number and mass transfer coefficient are reported in Table 5.9. From these results it can be concluded that the effect of mass transfer coefficient on the saturation time and hence, breakthrough time was negligible under the existing operating conditions. Similarly, the pore diffusion coefficient was also calculated to be approximately constant at 1.14 x 10^{-7} m^2/s over the entire range of flow rate. Therefore, decrease in breakthrough time and the total adsorption time with the increase in flow rate is attributed to the kinetic rate, which was controlled by the total amount of VOC reaching the surface of the fiber, as also found in the case of concentration effects. Table 5.9 also lists the numerical values of Schmidt number, dispersion coefficient and effective diffusivity, etc.

5.4 Effect of sorbent amount:

To study the effect of weight of the adsorbing materials (ACF), the experiments were carried out at three different amounts of ACF: 3, 5 and 9 g. These amounts of ACF sample corresponds to 1, 2 and 3 number of wraps, respectively. The inlet gas concentration and flow rate were kept constant at 10000 ppm and 0.5 slpm, respectively. The bed temperature was maintained at 50 ^{0}C.

Figure 5.9 describes the VOC breakthrough data for the various amounts ACF sample. As observed from the figure, the breakthrough time increases from 5 to 16 min with increase in the weight of ACF from 5 to 9 g. The corresponding total adsorption times were observed to be 40 to 60 min, respectively. As also observed from figure 5.9, the breakthrough came almost instantly for 3 g of the sample, the total adsorption time being 30 min. The increase in the breakthrough time with increase in the sample amount is obviously due to increase in the total adsorption surface area for VOC adsorption. The breakthrough time and the total adsorption time for three different amounts of ACF samples are reported in Table 5.8.

Figure 5.9 shows that the model predictions agree well with the experimental results. However, at higher amount of ACF sample an overshoot is observed in the model predicted breakthrough curve, as also seen in the case of flow rate (Figure 5.7), which is attributed due to the computational error involved in numerical system used in the present work. As observed from Table 5.3 the values of

the adjustable parameters b and $C_{s\mu}$ were kept constant at 8.5 kPa^{-1} and 0.95 mmol/g, respectively for each case. However, at higher amount of ACF sample (9 g) a lower value of $C_{s\mu}$ (0.57 mmol/g) was required to explain the experimental data. This may again be attributed due to a poor choice of the correlation used in this work to characterize the radial dispersion coefficient over a very small thickness (0.13 cm) of the bed, as also described in the previous section.

5.5 Effect of BET surface area:

The previous breakthrough data obtained for the two types of ACF samples (Type-1 and Type-2) under different temperatures and concentrations consistently revealed that the breakthrough times and the total adsorption times for Type-2 sample having a BET surface area 1700 m^2/g were greater than that for Type-1 sample having a BET area of 1000 m^2/g. The superiority of type2 sample over Type1 is clearly attributed due to a higher specific surface area, responsible for gas adsorption. To elucidate the above observation the data are replotted in Figures (5.10-5.11), on a comparable format. Under these conditions, the gas flow rate was held constant at 0.5 slpm. In either case, the reactor was wrapped with 5 g of the adsorbent. Figures (5.10-5.11) compares the experimentally obtained breakthrough curves of toluene during adsorption by two types of ACF samples (Type-1 and Type-2). As observed from Figure 5.10, the breakthrough times and the total adsorption times are greater in case of Type-2 sample than those in the case of Type-1 under two different bed temperatures (30 and 50 ^{0}C). It is clear from Figure 5.10 that at the temperature of 50 ^{0}C the breakthrough time in the case of Type-1 ACF was less than 5 min in comparison with 20 min for the Type-2 ACF. Similarly, the times to reach the VOC inlet concentration were approximately 40 and 72 min, respectively. As observed from Figure 5.11, the breakthrough curves follow the same trend under two different VOC inlet concentrations (2000 and 10000 ppm), indicating superior performance of the ACF with higher BET surface area than the ACF with relatively lower BET surface area.

5.6 Comparative adsorption performance of packed bed and perforated bed reactor:

Figure 5.12 compares the experimental breakthrough curves of toluene obtained from packed bed and perforated bed reactors during adsorption by ACF under identical

operating conditions. In the former, the ACF samples were packed in the bed after pretreatment, while in the later the ACF samples were wrapped over perforated teflon made reactor. In each case the experiments were carried out on 5 g of the ACF sample and at a constant gas flow rate of 0.5 slpm. The temperature of the bed in both cases was maintained constant at 50 °C. At the inlet concentration of 10000 ppm the breakthrough time in the case of packed bed was observed to be significantly higher (40 min) in comparison with that in the case of perforated bed (15 min), corresponding to a total adsorption time of 90 and 50 min, respectively. The same trend was also observed for a lower inlet VOC concentration i.e 4000 ppm. Hence, from the above observation it can be concluded that the adsorption by ACF in the packed form is much more effective than that by the ACF wrapped over the perforated teflon reactor under the identical operating conditions. The superiority of the ACF sample in packed form relative with that wrapped over the perforated reactor may be attributed due to sufficient time of contact between VOC in the laden gas and the adsorbent materials in the case of former than later. In the case of packed bed, residence time is $\dfrac{L}{V_0}$ which is much larger than $\dfrac{bed\ thickness}{V_r}$ in the case of perforated bed reactor. However, it is due to the ease of regeneration of saturated/equilibrated ACF by electrical heating on the ACF wrapped over the reactor that the later type of arrangement is generally preferred.

5.7 Comparative adsorption performance of granular activated carbon (GAC) and ACF:

Figure 5.13 compares the experimental breakthrough curves of toluene during adsorption by ACF and GAC under identical operating conditions. In either case, the reactor was packed with 10 g of the adsorbents (ACF or GAC). Due to difference in their bulk density and therefore, in the length of the bed, the bed porosity was calculated to be 0.68 and 0.37 for ACF and GAC, respectively. The temperature of the packed bed was held constant at 45 ° C. The toluene concentration in the inlet gas was 4000 ppm, which corresponded to approximately −10 ° C of the bottle temperature. As observed from the figure, the breakthrough times in the case of AFC are larger than those in the case of GAC under three N_2 flow rates (0.5, 1.0 and 1.5 slpm), indicating superior performance of the former than the latter. At higher flow rate (i.e. 1.5 slpm), the breakthrough time in the case of GAC was observed to be less than 5 min in comparison with 35 min for ACF. Similarly, the times to asymptotically reach the VOC inlet concentration were approximately 5 and

comparison with GAC is also reported elsewhere (Inagaki, 2000). The superiority of ACF over GAC in capturing VOC is attributed to a large number of micropores on their surfaces, responsible for the gas adsorption. The model developed in this study was also applied to simulate the experimental breakthrough curves. Figure 5.13 compares the model results with the adsorption data of toluene for both ACF and GAC. The model predictions are observed to be in good agreement with the data. As pointed out in the theoretical analysis the values of the adsorption/desorption constants required in the model were obtained from a previous work and the remaining parameters were calculated based on the existing operating conditions.

The adsorption experiments were also carried out at relatively higher concentration, i.e. 50000 ppm (5%) to determine the relative performances of ACF and GAC in adsorbing the organic pollutant. This concentration corresponds to the liquid toluene temperature of 30 °C. As observed from the breakthrough curves drawn on Figure 5.14 for varying N_2 flowrates (0.2, 0.5, and 1 slpm) the breakthrough times for ACF were higher than the respective times for GAC under identical experimental operating conditions. The similar breakthrough characteristics were consistently observed under several other experimental conditions used in this study. Based on these results, it was concluded that ACF exhibited enhanced adsorption capacity for VOC in comparison with GAC for the same amount of the materials.

5.8 Effect of regeneration time on the adsorption performance of ACF:

In the present study, electrical heating was employed to regenerate the fibers saturated with VOC during adsorption. The details of the arrangement were previously described in the section on the experiment. A series of the test runs were carried out to determine the optimum regeneration conditions, including regeneration time and DC voltage. For each case the regenerated fiber cloth was re-subjected to the adsorption test to determine its adsorption performance following regeneration. Figure 5.15 describes one of such results obtained on the breakthrough of the ACF regenerated for different regeneration times. The adsorbent was equilibrated with 8000 ppm of toluene prior to regeneration. The voltage was maintained constant at 40 V. The corresponding temperature of the cloth was measured to be 150 ° C. As observed from the figure, there is insignificant difference between the adsorption profiles of the fiber cloth regenerated for 15 and 30 min. The adsorption characteristics of the fiber clothes which were regenerated for at least 45 min are, however, found to improve, resulting in increase in the breakthrough time. The adsorption profiles of ACF regenerated for 60 min are observed to be approximately

identical to those of a fresh ACF. Therefore, in this study a regeneration time of 60 min was chosen to be optimum for the maximum removal of the adsorbed VOC. During the regeneration period, the current gradually increased from an initial value of 1 A to 3 A, indicating decrease in the electrical resistance of the fiber from 40 Ω to approximately 13 Ω, as the adsorbed VOC was gradually removed from the fabric due to heating.

5.9 Model parametric study:

Model simulation of a large-scale VOC emission:

After validation of the model developed in the study, the simulations were carried out for an adsorption bed required to control a large scale VOC emission from an industry. A reactor of 0.3 m I.D and 1.0 m height, containing 40 kg of ACF sample wrapped over a perforated reactor was assumed. The bed temperature was assumed to be 50 ^{0}C and the inlet concentration 5000 ppm. Figure 5.16 shows the breakthrough curves for the VOC laden flue gas at varying flow rates of 250, 500 and 750 slpm. The corresponding breakthrough times are observed to be 300, 200 and 120 min, respectively. Thus with the help of above-simulated results, change over time to put a bed of fresh adsorbent materials can be estimated. In the present case if the flow rate is 250 slpm a changeover time after approximately 5 hr is required. Hence the simulated results are useful in designing an industrially sized adsorber.

Effect of dispersion coefficients:

Figure 5.17 describes the effect of dispersion coefficient on VOC breakthrough curve by model predictions. As discussed in section 5.3 the correlation available for determining axial dispersion coefficient in a packed bed was used in the present study to characterize the radial dispersion coefficient over a very small thickness (0.13 cm) of the fabric bed. This necessitates studying the effects of dispersion coefficient on the VOC breakthrough curve under identical operating conditions. The simulations were carried out for different dispersion coefficients ranging from 2.92 x 10^{-3} to 2.92 x 10^{-8} m^2/s (difference in five orders of magnitude). As observed from the plots on Figure 5.17, the breakthrough times and the total adsorption times were approximately same in all the cases for which the value of dispersion coefficient was chosen $\geq$ 2.92 x 10^{-5} m^2/s. However, as the dispersion coefficient was decreased to 2.92 x 10^{-6} m^2/s, the breakthrough time was observe to increase to 10 min, without any significant change in total adsorption time (37 min). With further decrease in the value of dispersion coefficient by one order of magnitude (2.92 x 10^{-7} m^2/s) the breakthrough time

significantly increased to 20 min and the total adsorption time was found to decrease to 28 min. As also observed from Figure 5.17, with further decrease in the dispersion coefficient (2.92×10^{-8} m^2/s) the breakthrough curve became sharp with abrupt rise in the concentration level. Beyond this a marginal increase and decrease in the breakthrough time and total adsorption, respectively time was observed.

The above effects (abrupt rise in the concentration level at smaller values of the dispersion coefficient) may be attributed due to high inertial effects in the bed. As seen from equation 3.17 in the theoretical analysis section the intermediate coefficient C involves the dispersion coefficient term. At lower value of dispersion coefficient C becomes very small. As a consequence the inertial effects in the bed become predominant in comparison with the dispersion effects. Hence, the bed appears to be saturated with VOC, with the exit concentration becoming equal to the inlet concentration level.
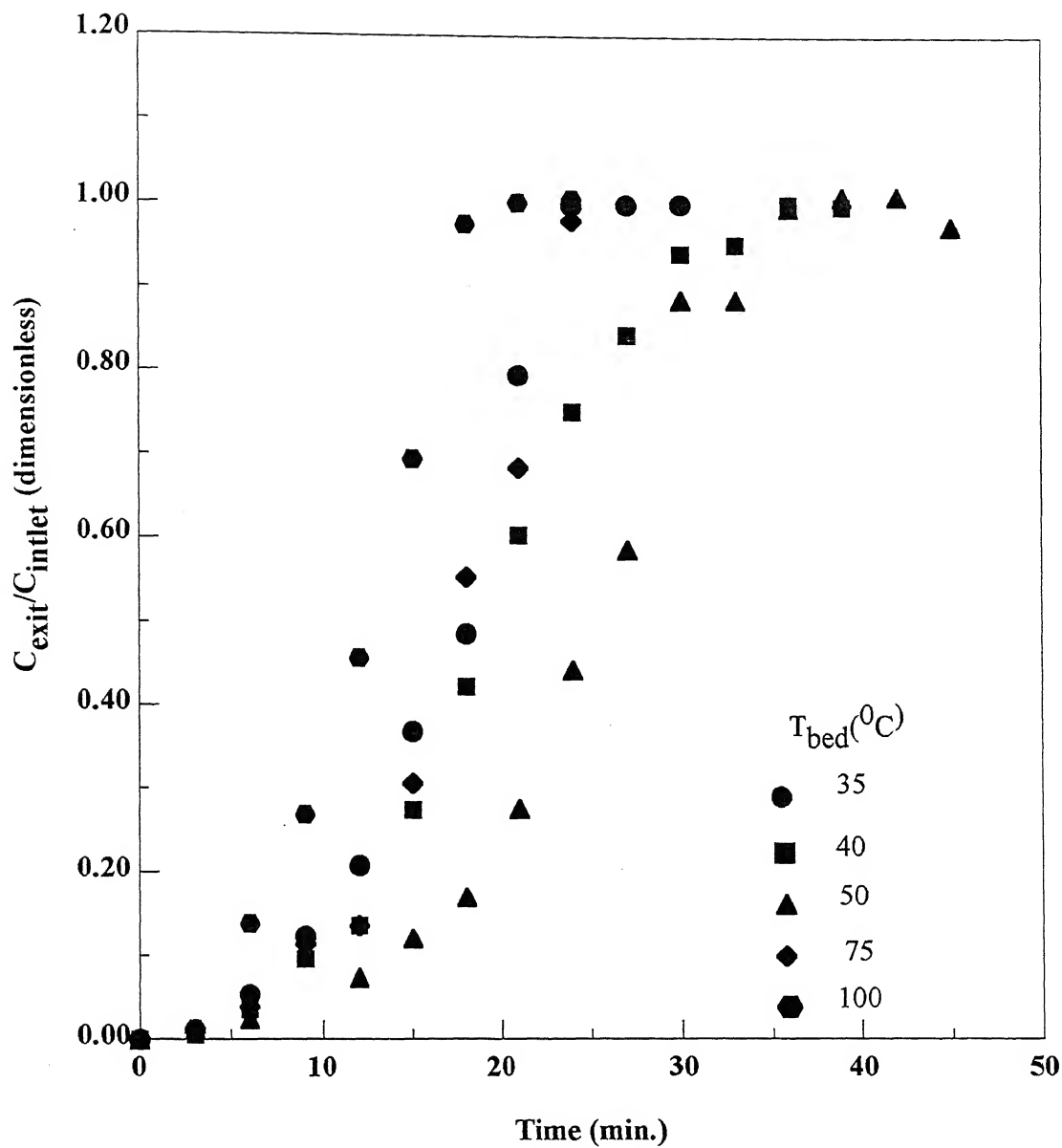
Fig.5.1 : Effect of bed temperature on breakthrough of toluene over ACF-Type 1
(W= 5.0 g, Q_{N_2}= 0.5 slpm, C = 10000ppm)
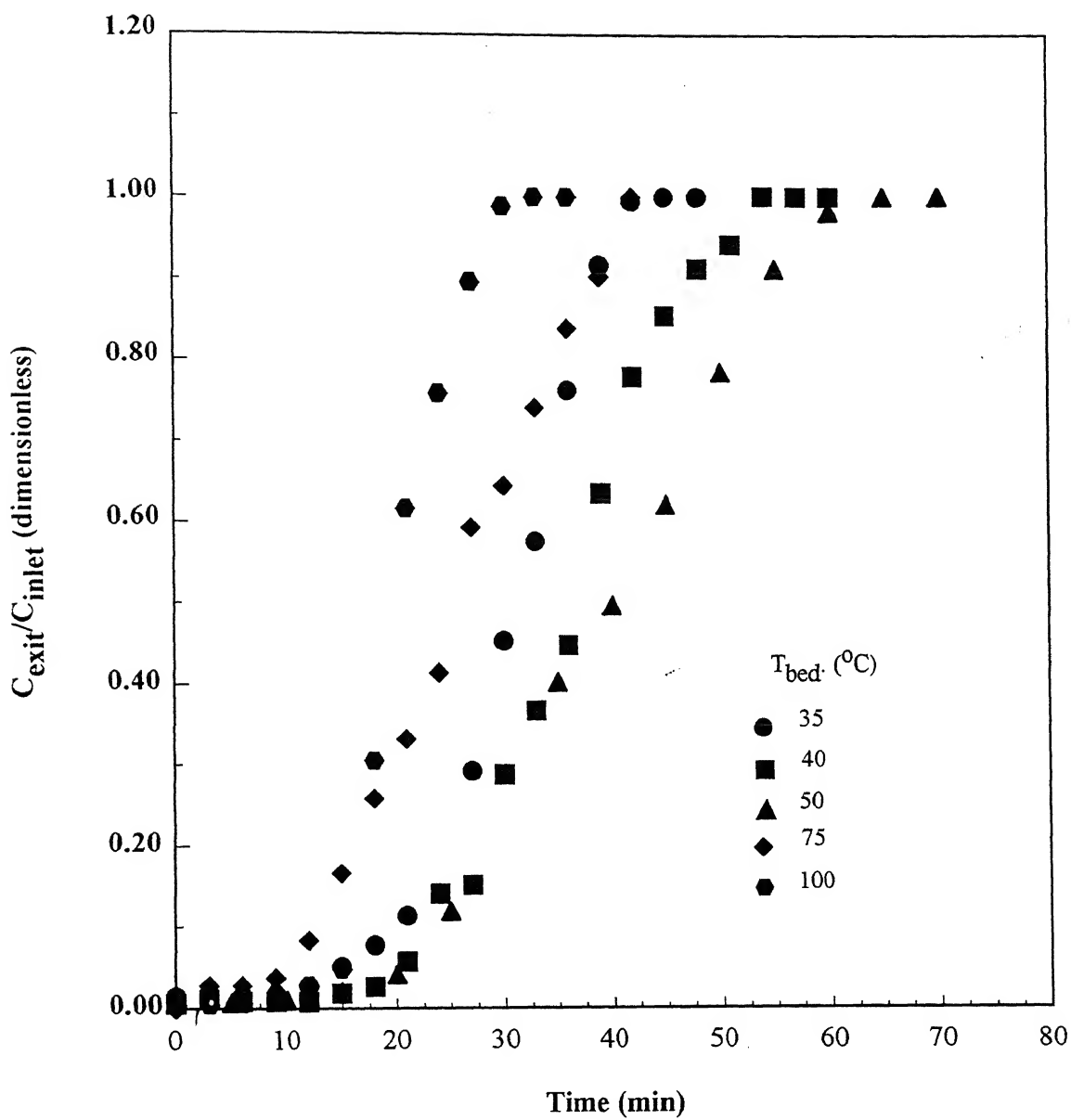
Fig.5.2 : Effect of bed temperature on breakthrough of toluene over ACF-Type 2
(W= 5.0 g, Q_{N_2} = 0.5 slpm, C = 10000 ppm)

40
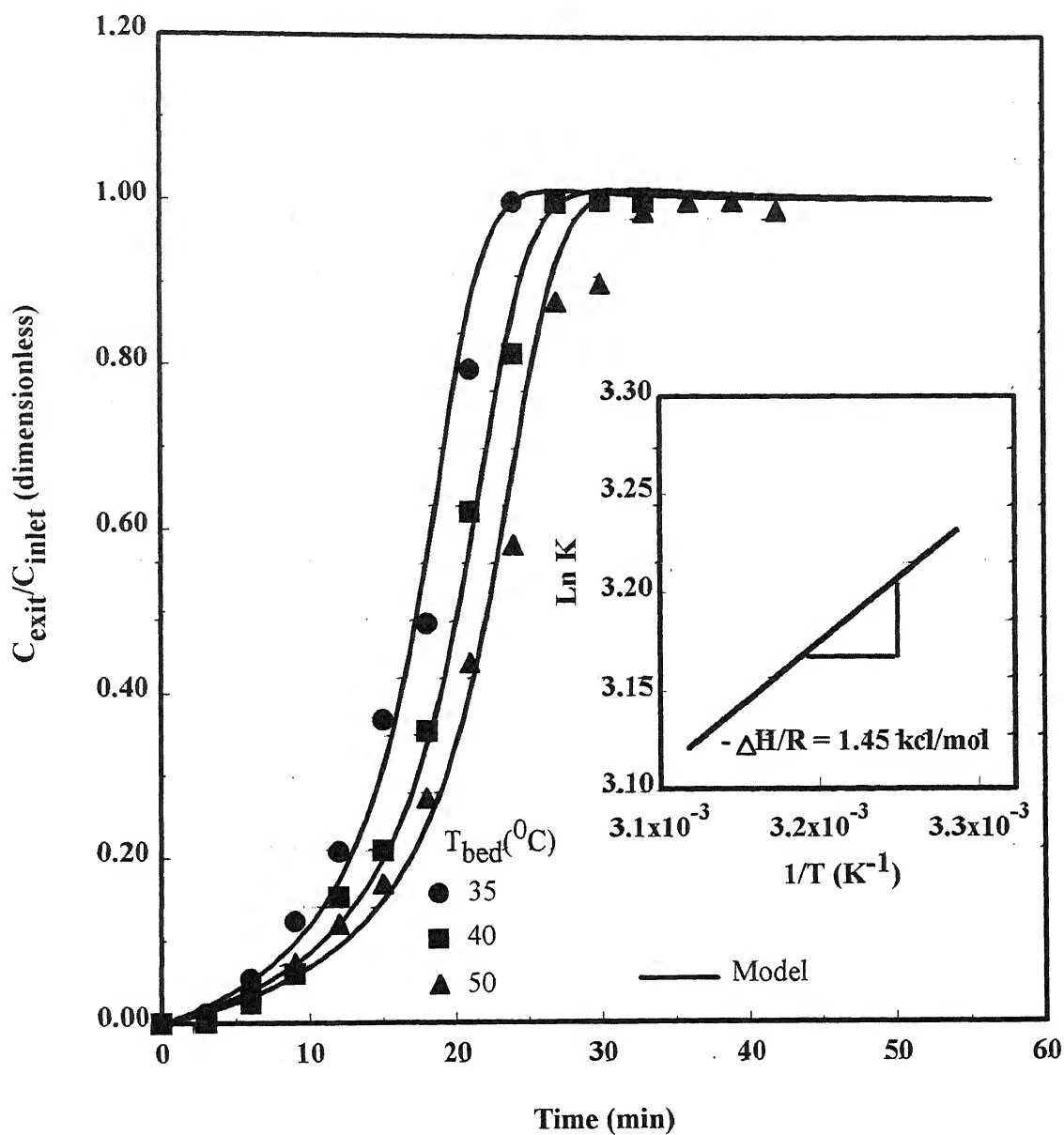
Fig 5.3 : Comparison of model predictions and experimental data for effect of bed temperatur determination of heat of adsorption of VOC over ACF-Type 1
(W= 5.0 g, Q_{N_2} = 0.5 slpm, C = 10000 ppm)
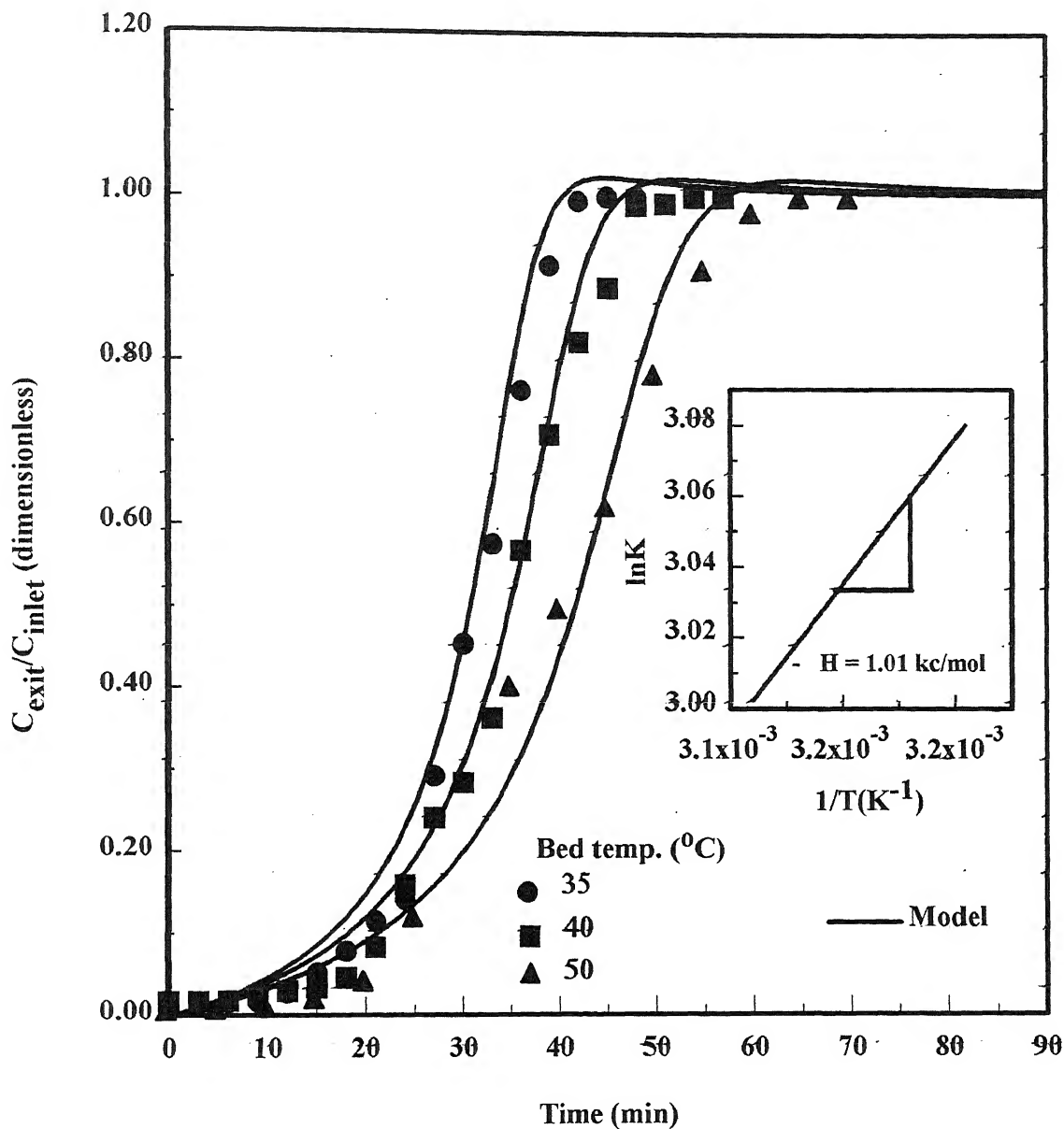
Fig 5.4 : Comparison of model predictions and experimental data for effect of bed temperature: determination of heat of adsorption of VOC over ACF-Type 2
(W = 5.0 g, Q_{N_2} = 0.5 slpm, C = 10000 ppm)
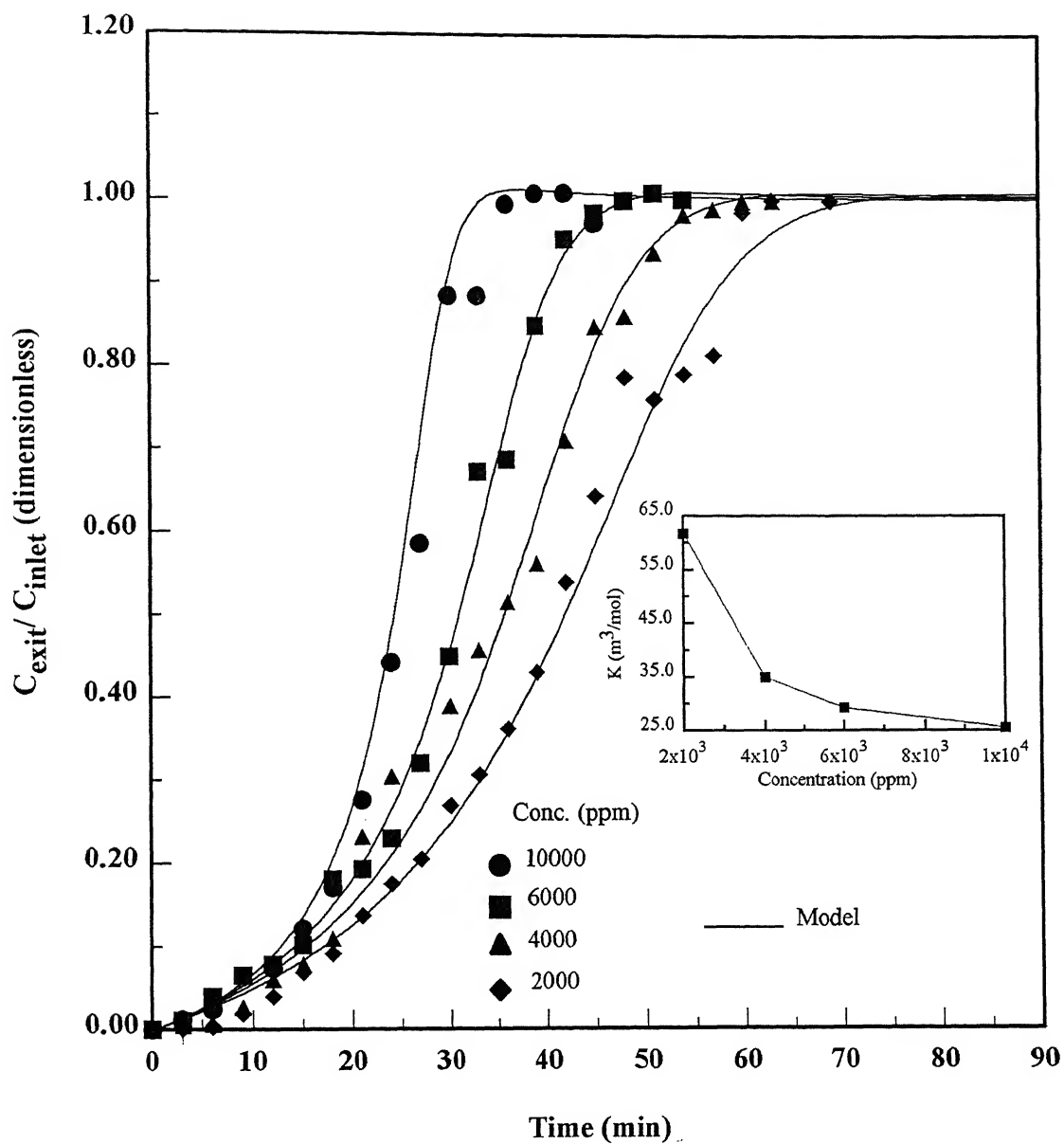
Fig.5.5 : Effect of concentration on breakthrough of toluene over ACF-Type1
(W = 5.0g, Q_{N_2} = 0.5 slpm, T_{bed} = 50^{0}C)
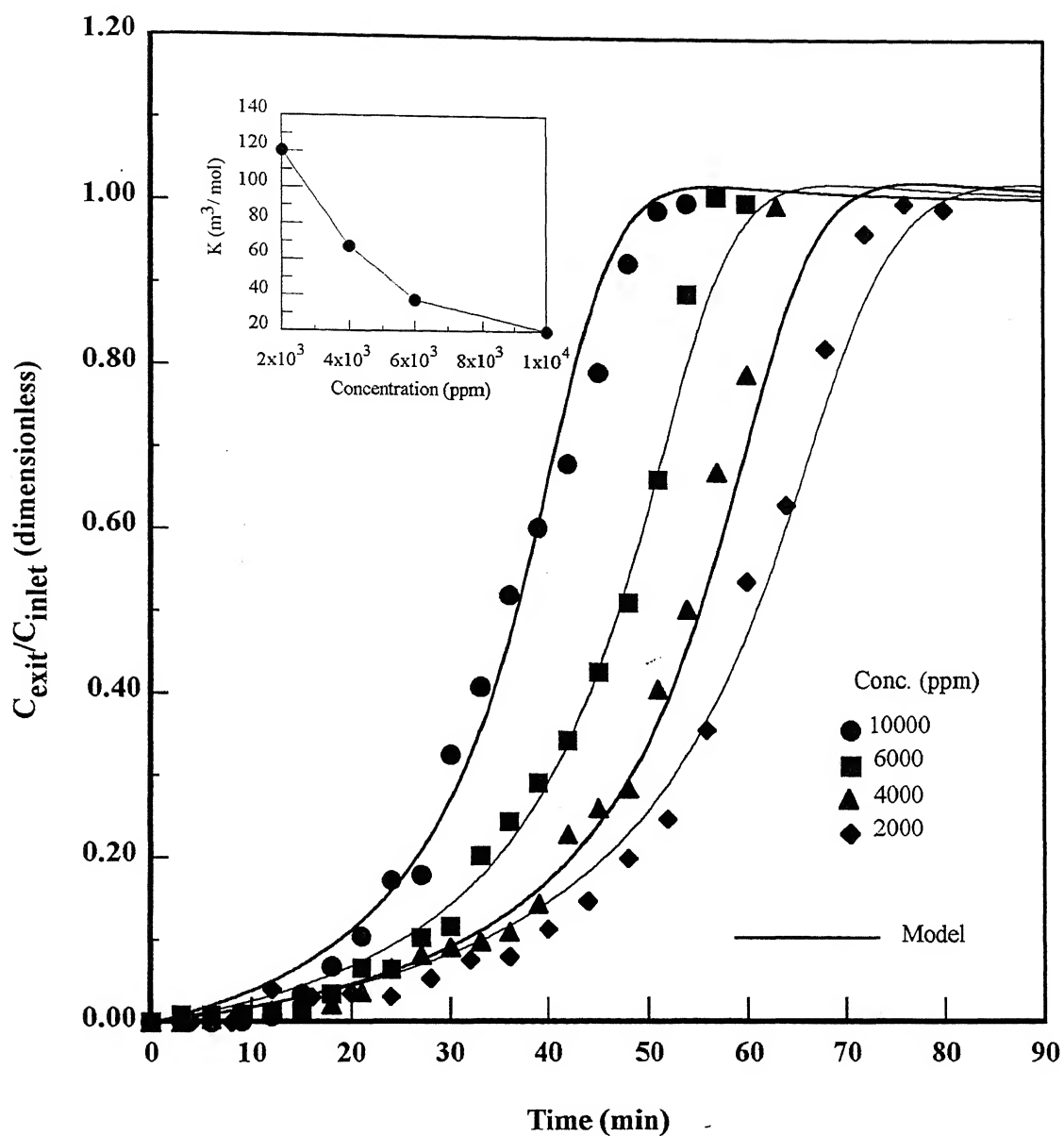
Fig. 5.6 : Effect of concentration on breakthrough of toluene over ACF-Type2
(W = 5.0 g, Q_{N_2} = 0.5 slpm, T_{bed} = 50^{0}C)
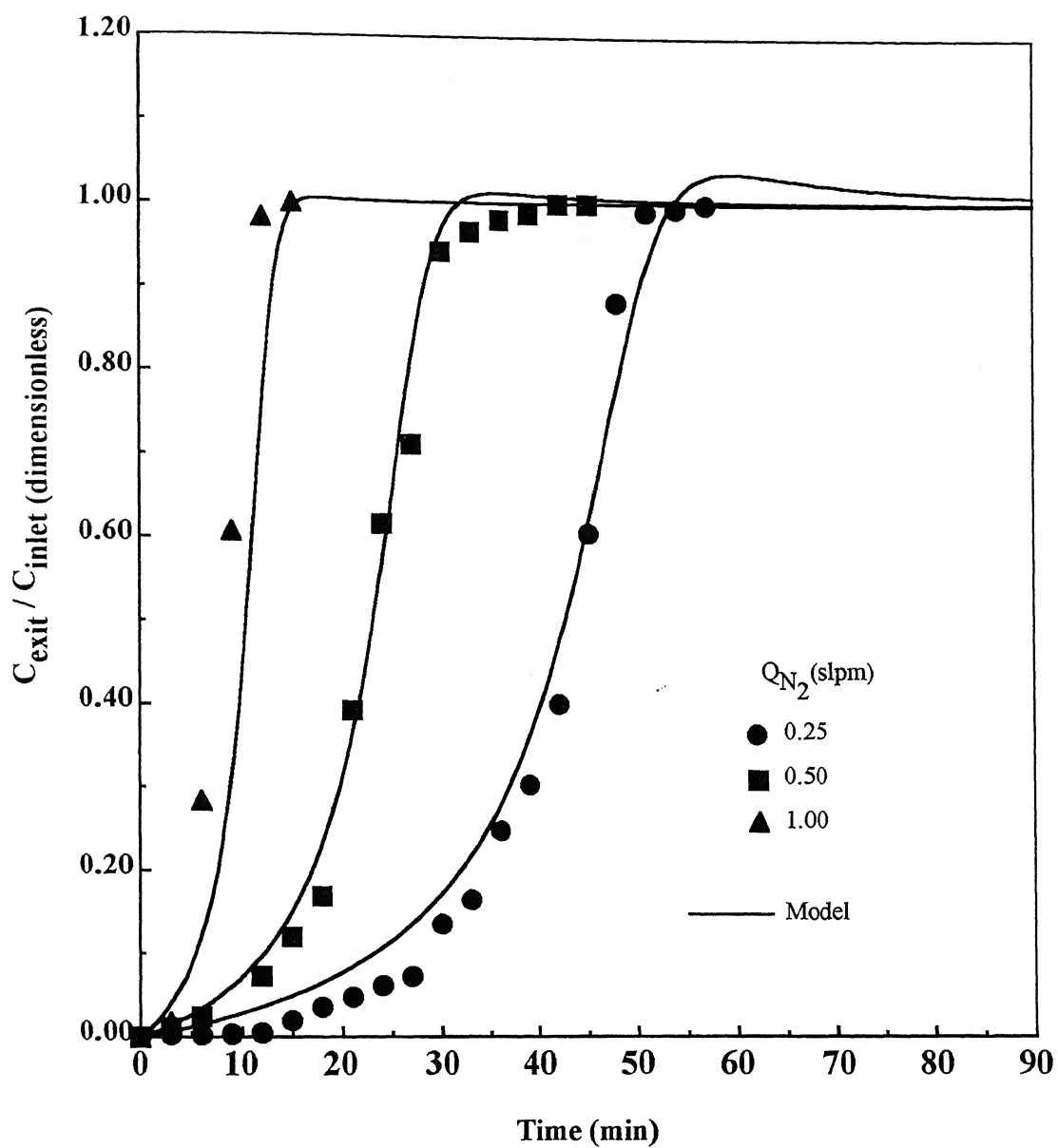
Fig.5.7 : Effect of gas flowrate on breakthrough of toluene over ACF-Type1
(W= 5.0g, C = 10000 ppm, T_{bed} = 50^0C)
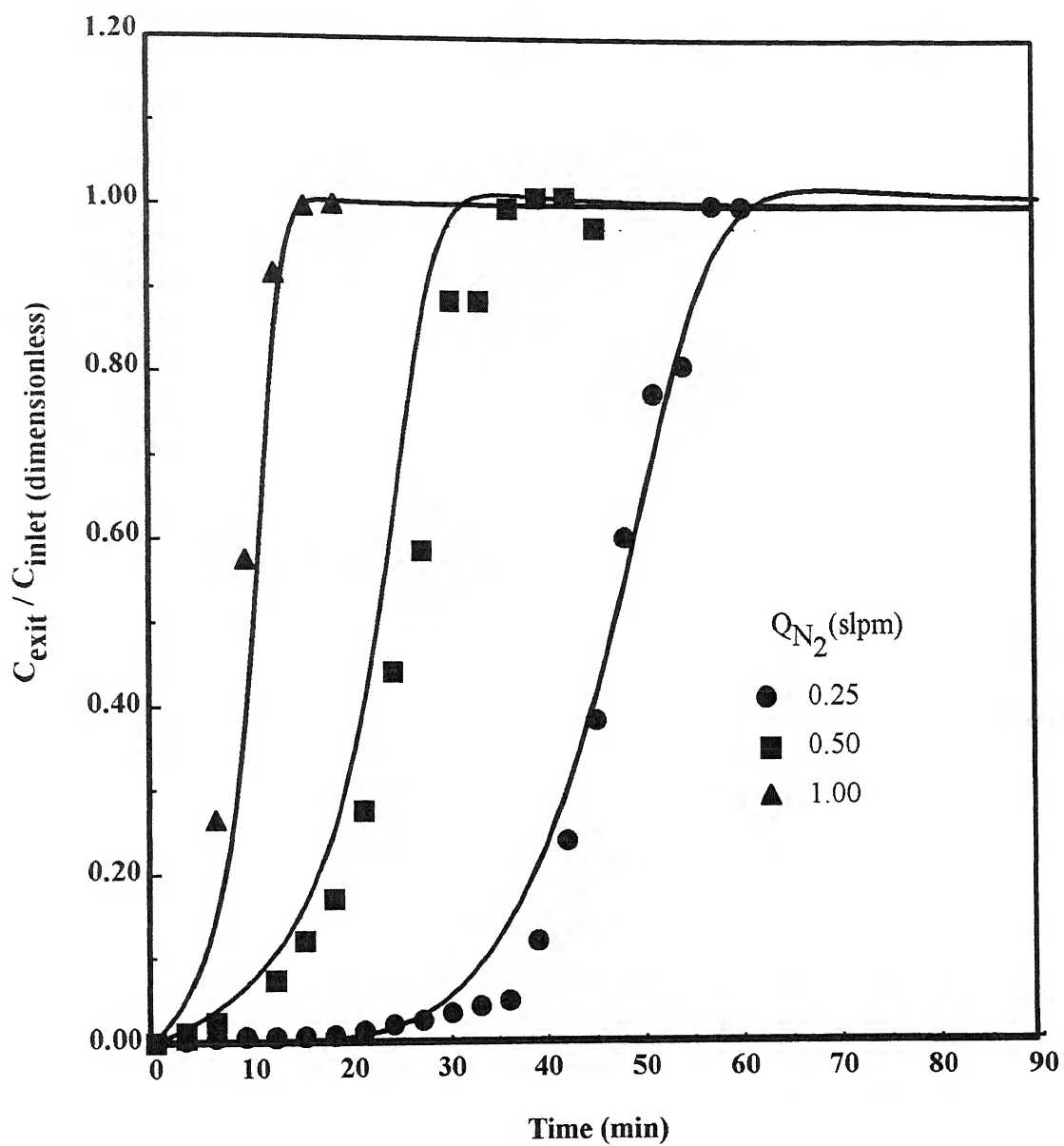
Fig. 5.8: Effect of gas flowrate on breakthrough of toluene over ACF-Type1
(W= 5.0g, C = 10000 ppm, T_{bed}= 50^0C)
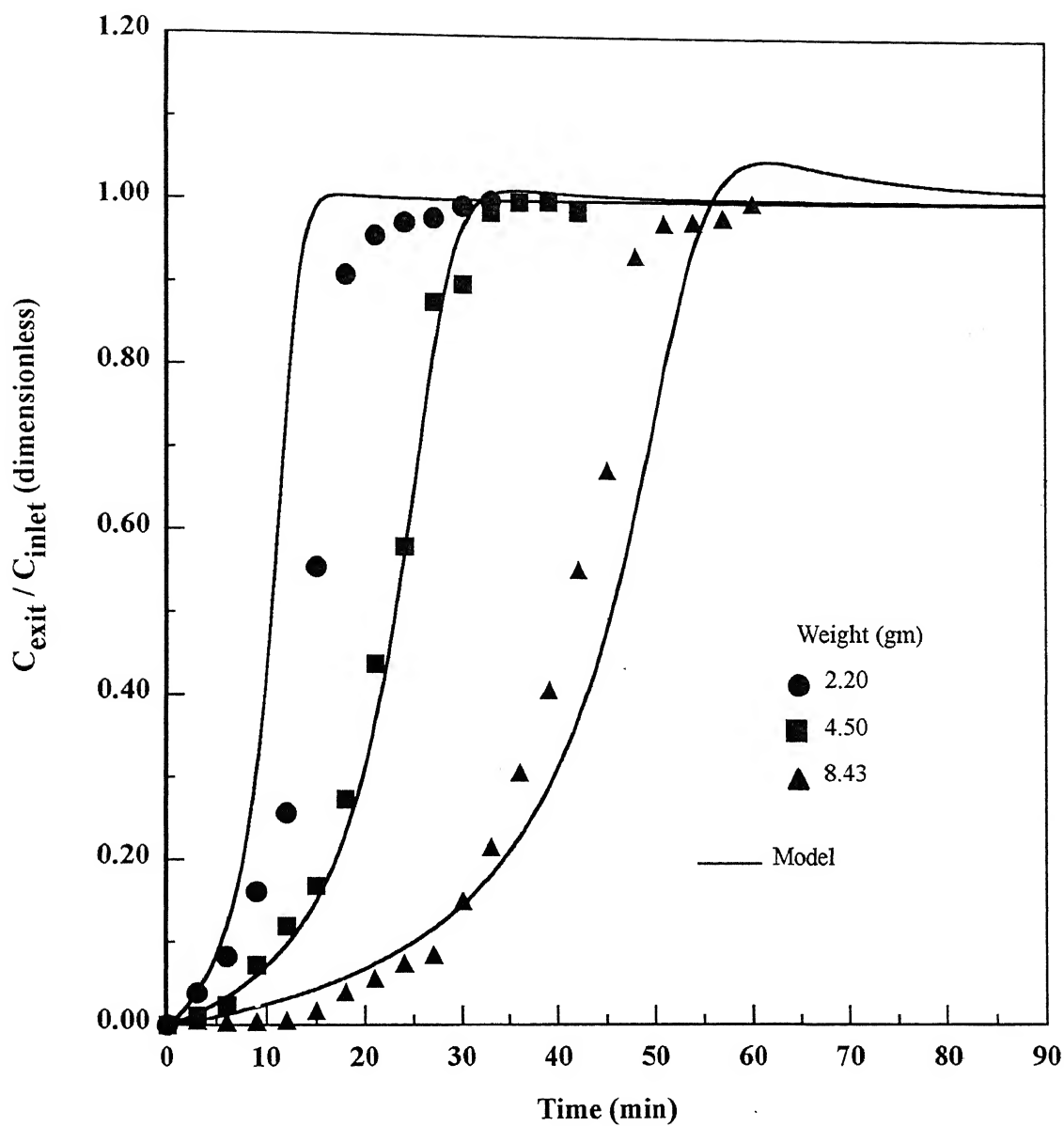
Fig. 5.9: Effect of weight on breakthrough of toluene over ACF-Type1
$(Q = 0.5 \text{ slpm}, C = 10000 \text{ ppm}, T_{bed} = 50^0C)$

47
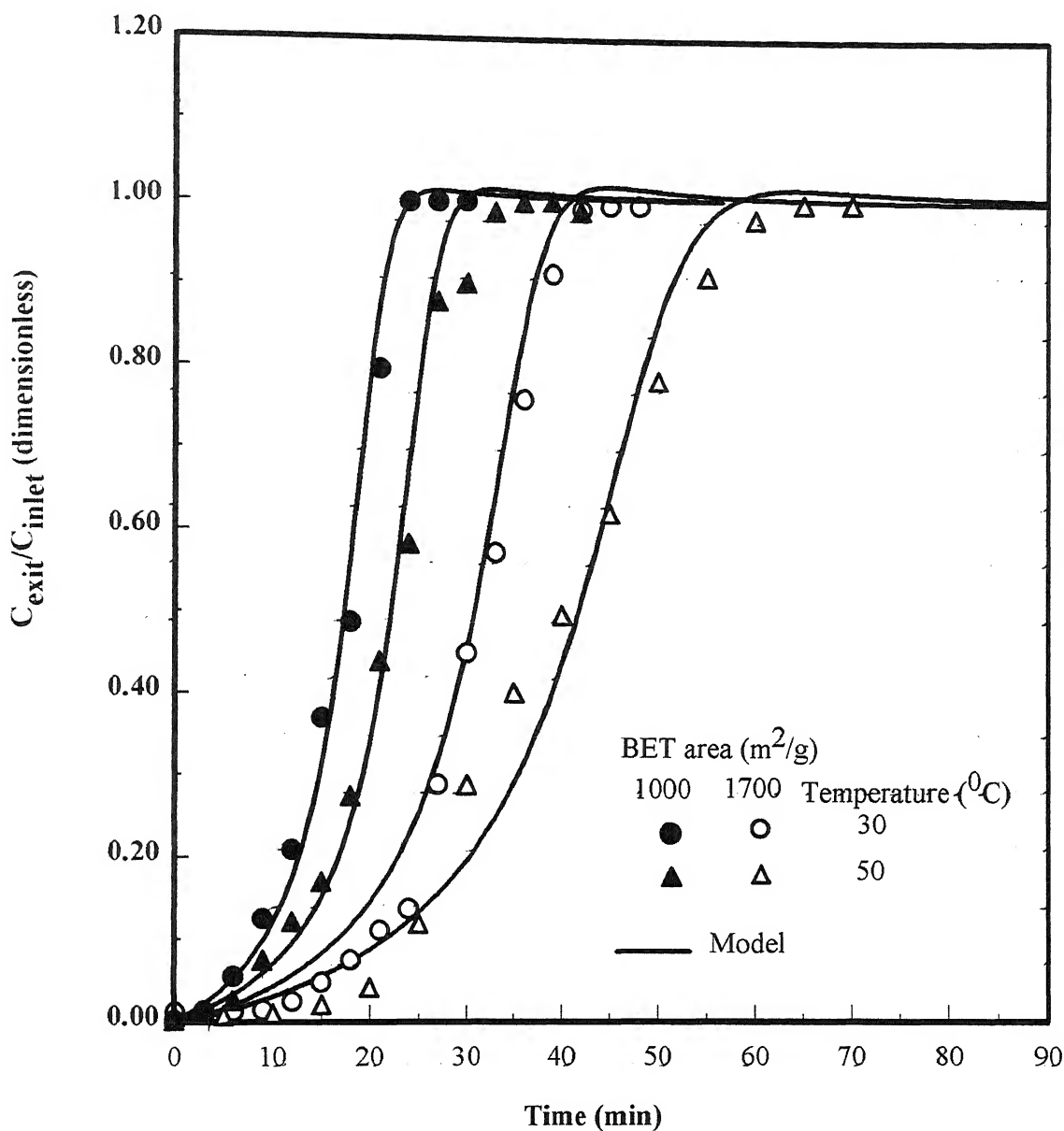
Fig.5.10 : Effect of BET surface area on breakthrough of toluene over ACF
under different bed temperatures.
(W = 5.0 g, Q_{N_2} = 0.5 slpm, C = 10000 ppm)

48
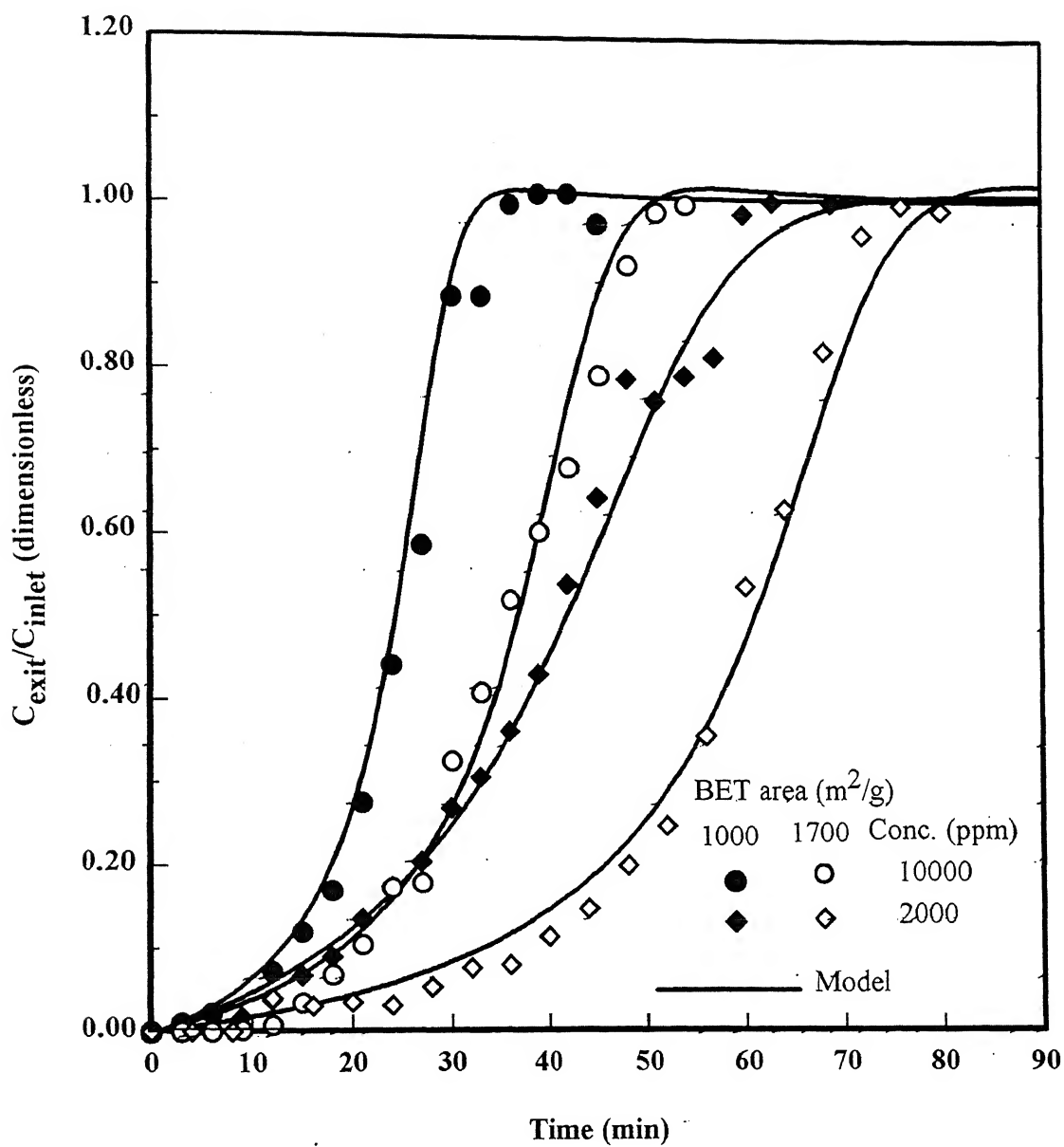
Fig.5.11 : Effect of BET surface area on breakthrough of toluene over ACF
under different concentration levels

$(W = 5.0g, Q_{N_2} = 0.5slpm, T_{bed} = 50^0C)$

49
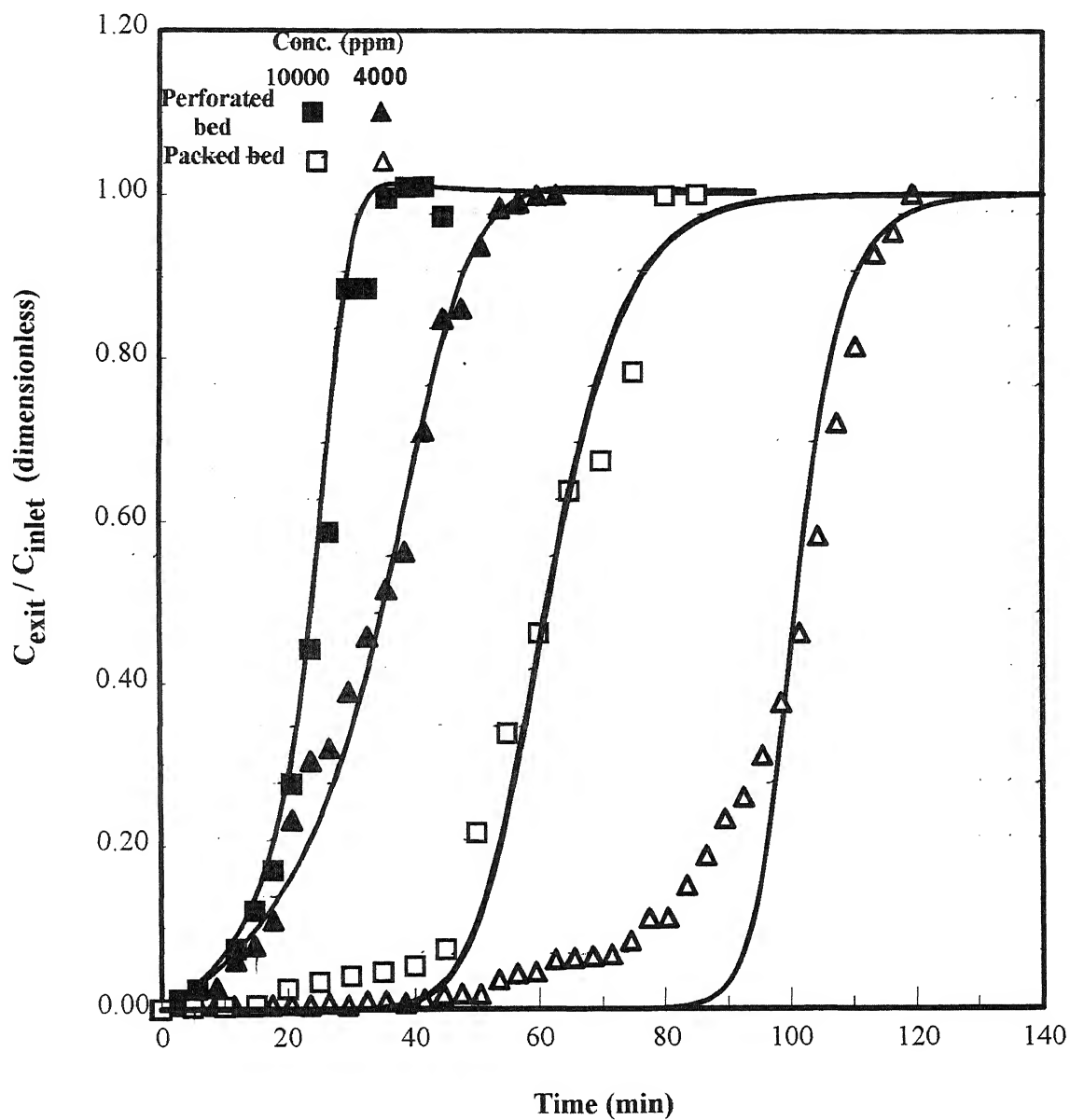
Fig.5.12: Comparison of adsorption performance between packed and perforated bed of ACF

$(W = 5.0 \text{ g}, Q_{N_2} = 0.5 \text{ slpm}, T_{bed} = 50^{o}C)$
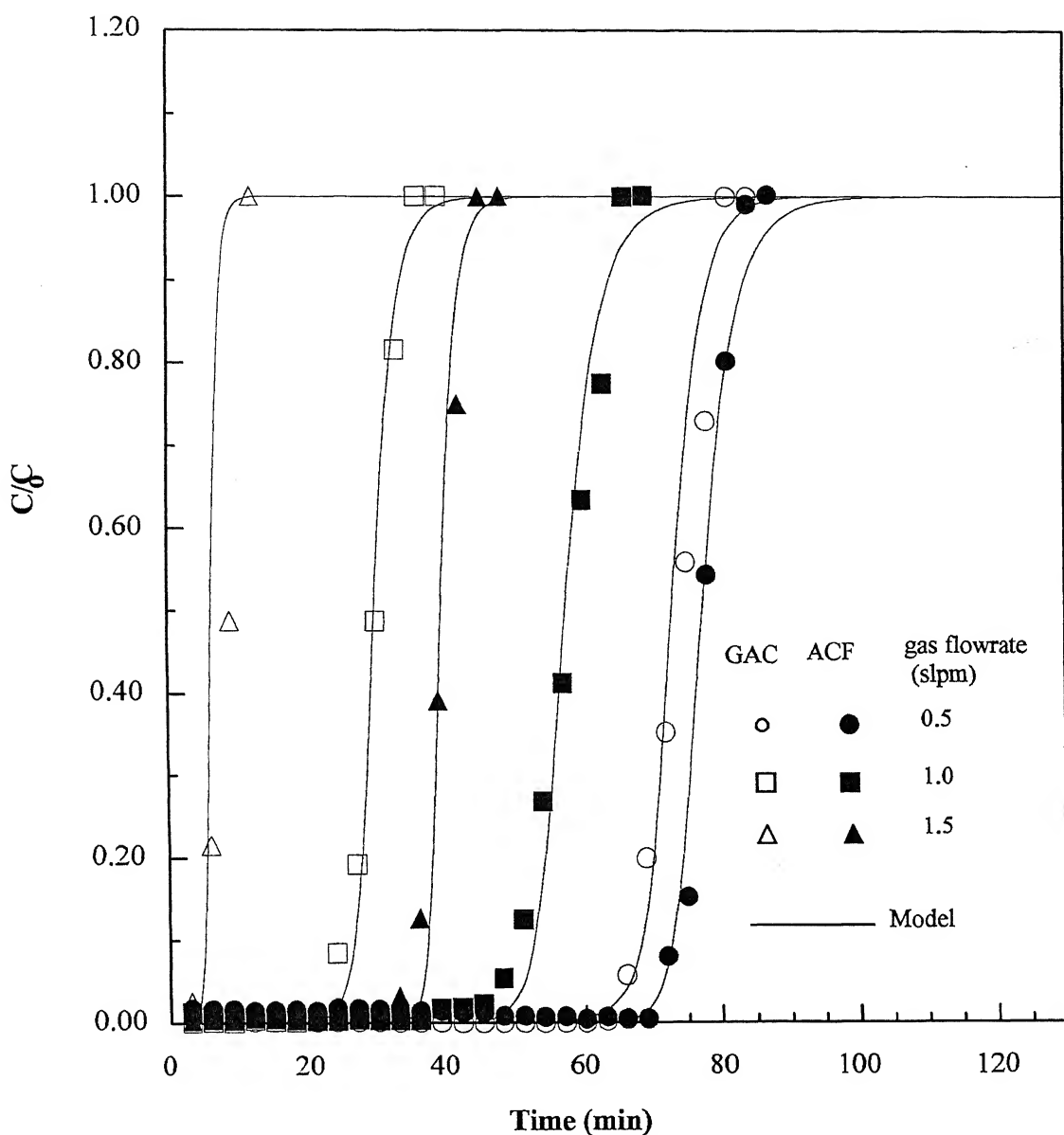
Fig 5.13: Breakthrough characteristics of toluene: Data and model predictions.
$(T_{bed} = 45^oC, C_{inlet} = 4000$ ppm, W = 10 gm, L = 20 cm, bed porosity = 0.68)
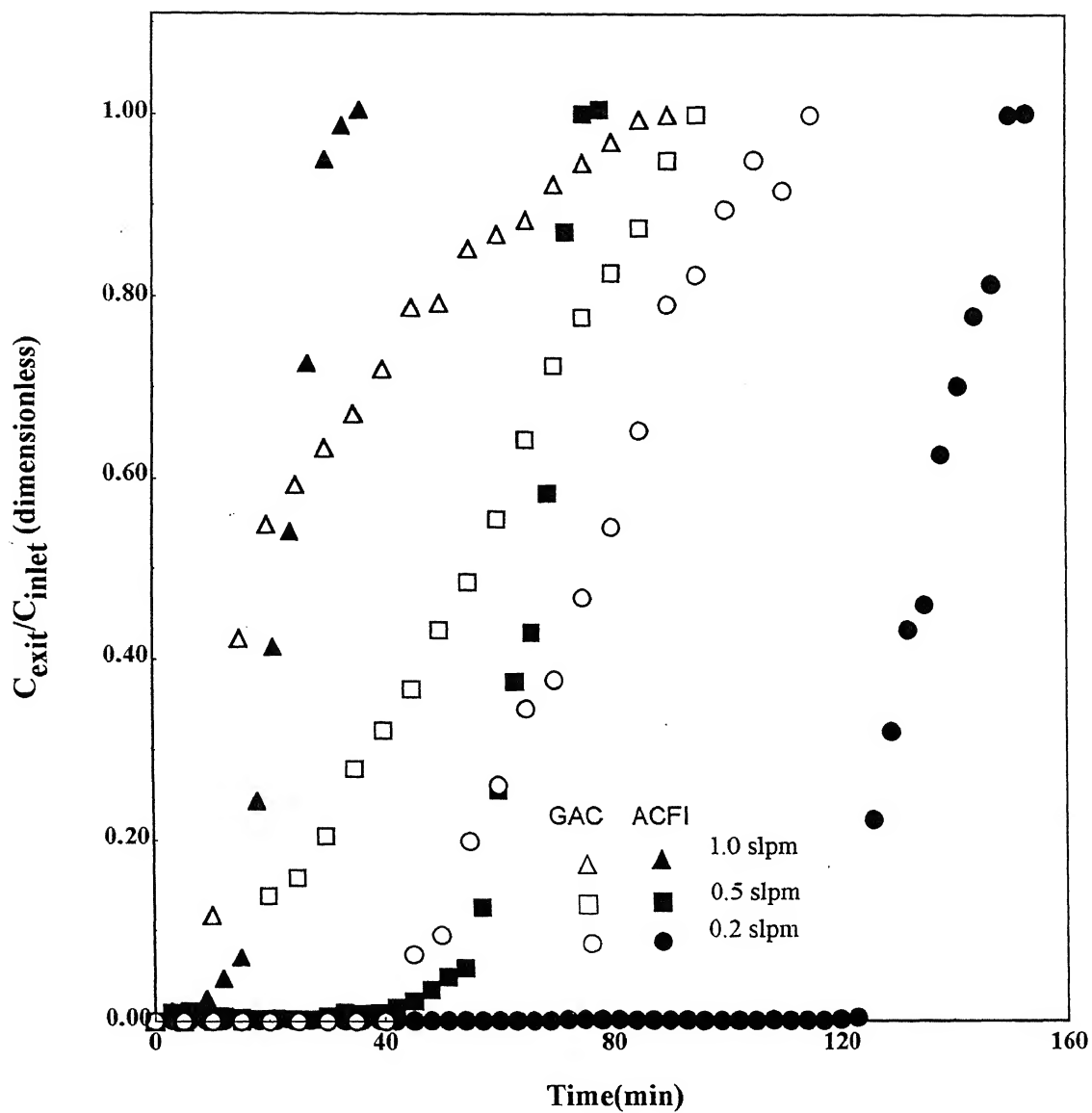
Fig. 5.14: Comparative adsorption performance of granular activated carbon and ACF (W = 10 g, T_{bed} = 45°C, bed porosity = 0.68, C_{inlet} = 50000 ppm)
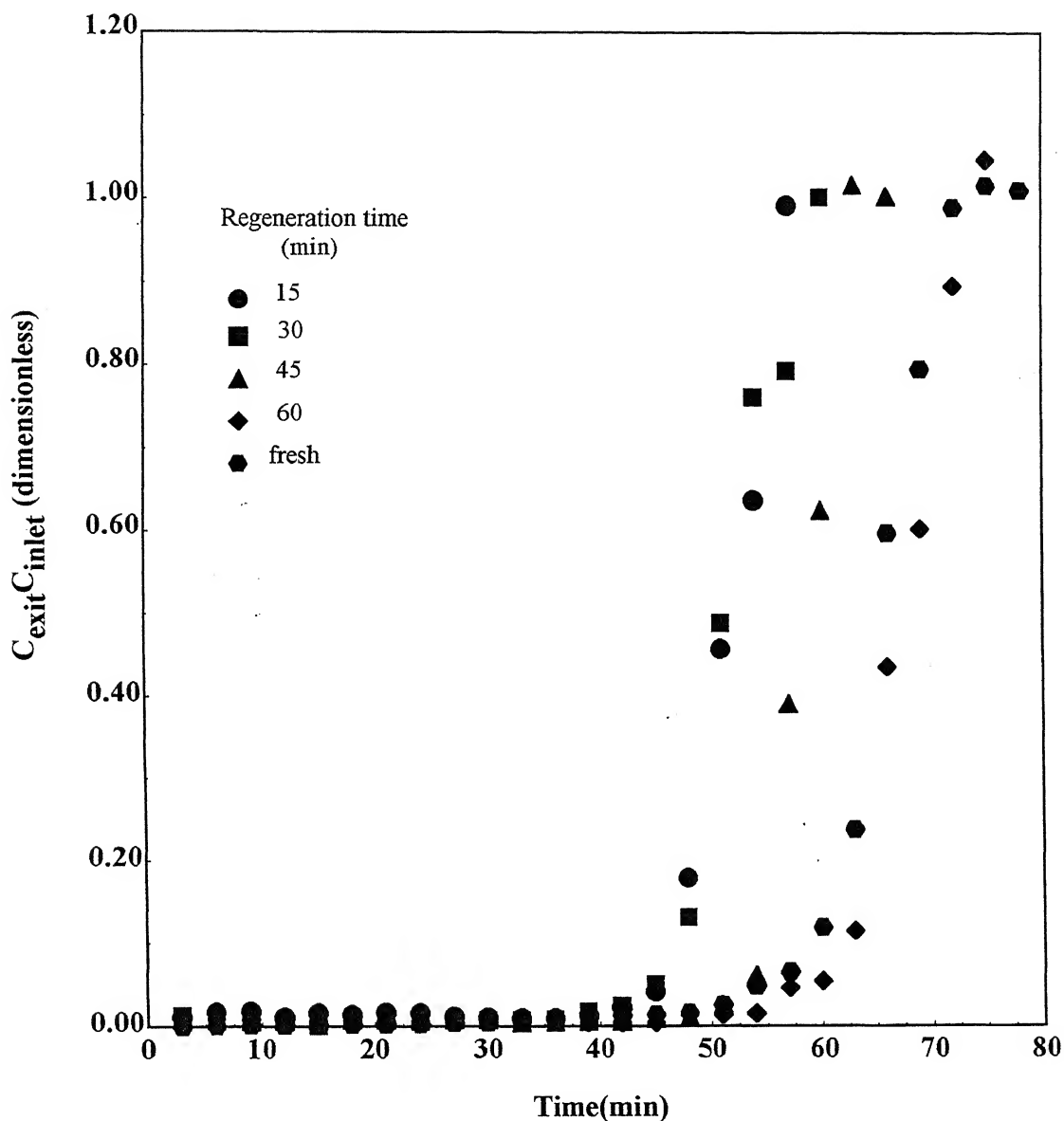
Fig. 5.15: Effect of regeneration time on adsorption time by ACF wrapped on perforated teflon reactor (Q = 0.2 slpm, W = 6.2 g, T_{bed} = 45 ^{O}C)

(Regeneration conditions: Q = 0.05 slpm, T_{bed} = 150 ^{O}C, Volts = 40 v)
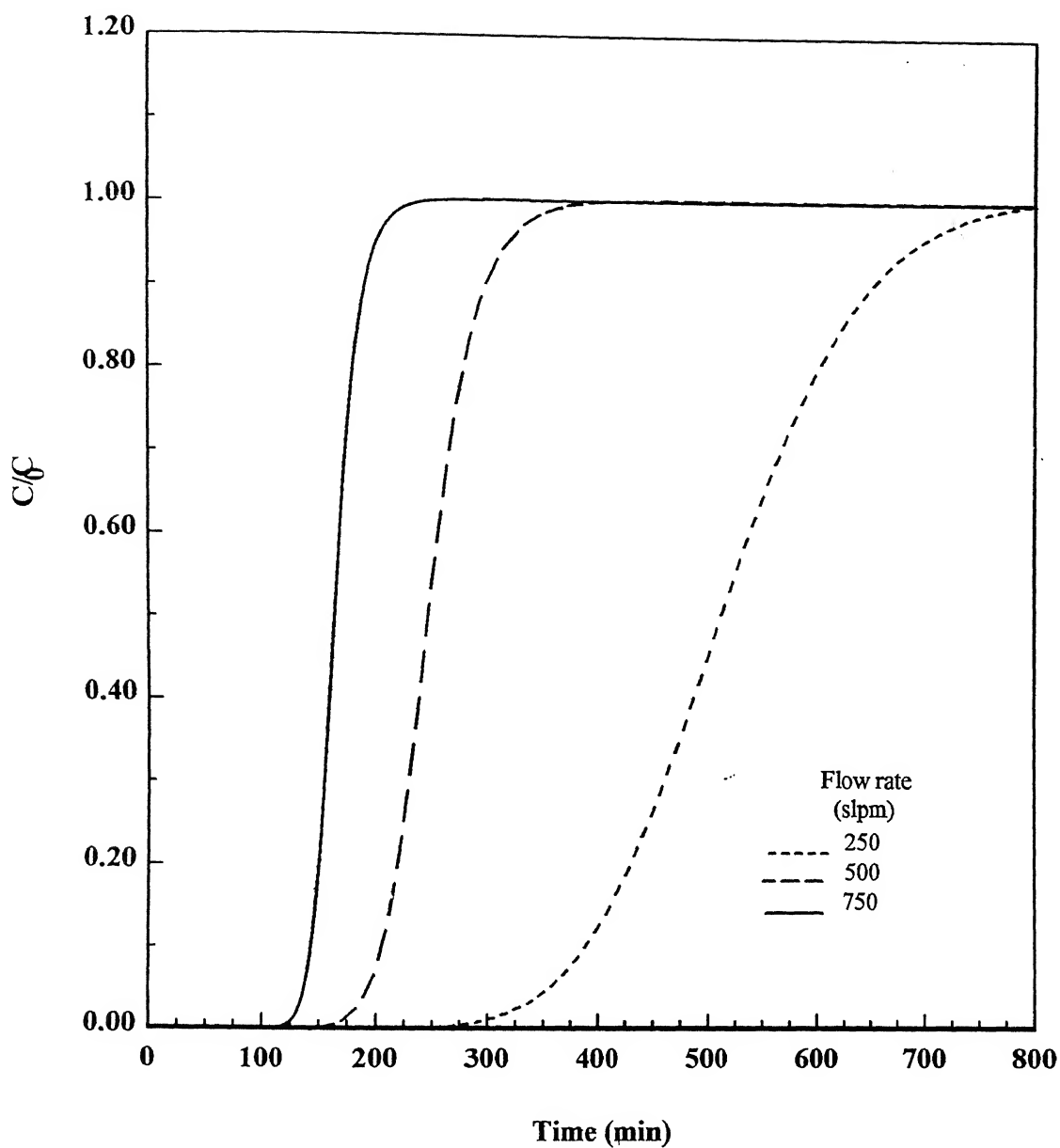
Fig. 5.16: Model predictions for VOC removal on an industrial scale
(L = 1.0 m, I.D = 0.3 m, W = 40 kg, T = 50 ^{0}C,
C_{inlet} = 5000 ppm, thickness = 0.254 m)
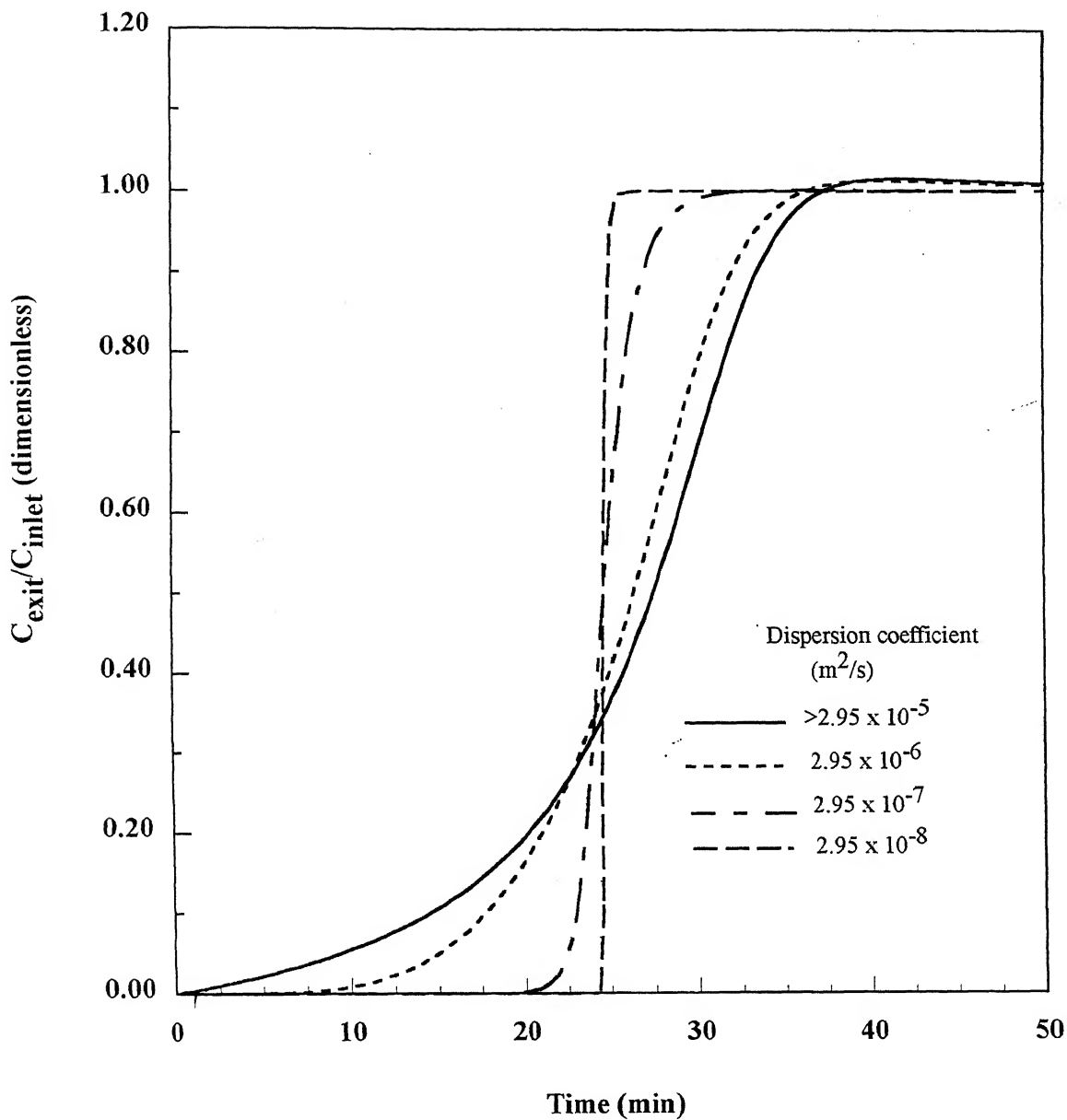
Fig. 5.17: Effect of dispersion coefficient on VOC breakthrough
(R_p = 3 x 10^{-9} m, K_m = 41.247 m/s, D_m = 9.47 x 10^{-6} m^{2}s)
(T = 50^{0}C, C_{inlet} = 10000 ppm, W = 5 g)

55

Sample	S. No.	Bed temperature (^{0}C)	Breakthrough time (min)	Total adsorption time (min)
ACF-Type 1 (Procured locally)	1	35	7	30
	2	40	7	40
	3	50	10	50
	4	75	7	25
	5	100	3	21
ACF-Type 2 (Imported)	6	35	20	50
	7	40	20	60
	8	50	20	70
	9	75	12	42
	10	100	8	40

Table 5.1: Breakthrough time and total adsorption time of two different type of ACF samples at different bed temperatures.

Temperature(^{0}C)	K (m^3/mol)	
	ACF (Type-1 sample) (Procured locally)	ACF (Type-2 sample) (Imported)
35	25.60	21.76
40	23.94	20.95
50	22.816	20.14

Table 5.2: Adsorption equilibrium constant at various bed temperatures

Fig. 5.3 : Effect of bed temperature on Breakthrough of Toluene over ACF
(W = 5 g, Q_{N2}= 0.5 slpm, C = 10000 ppm)

Temperature(^{0}C)	b (1/kPa)	$C_{s\mu}$ (mmol/gm)
35	10.0	0.75
40	9.2	0.85
50	8.5	0.95

Fig. 5.5 : Effect of concentration on breakthrough of toluene over ACF
(W = 5 g, Q_{N2}= 0.5 slpm = 0.5 slpm, T_{bed} = 50°C)

Concentration (ppm)	b (1/kPa)	$C_{s\mu}$ (mmol/gm)
2000	23.0	0.38
4000	13.0	0.64
6000	12.0	0.80
10000	8.5	0.95

Fig. 5.7 : Effect of gas flowrate on breakthrough of toluene over ACF
(W = 5 g, C = 10000 ppm, T_{bed} = 50°C)

Flowrate (slpm)	b (1/kPa)	$C_{s\mu}$ (mmol/gm)
0.25	8.5	0.95
0.50	8.5	0.95
1.00	8.5	0.95

Fig. 5.8: Effect of weight on Breakthrough of toluene over ACF
(Q = 0.5slpm, C = 10000 ppm, T_{bed} = 50°C)

Weight (g.)	b (1/kPa)	$C_{s\mu}$ (mmol/gm)
3	8.5	0.95
5	8.5	0.95
9	8.5	0.57

Table 5.3: Sips isotherm parameters for various experimental conditions
(Sample # ACF-Type1, N = 1.0)

Fig. 5.4 : Effect of bed temperature on Breakthrough of Toluene over ACF (W = 5 g, Q_{N2}= 0.5 slpm, C = 10000 ppm)		
Temperature(^{0}C)	b (1/kPa)	$C_{s\mu}$ (mmol/gm)
35	8.5	1.33
42	8.0	1.45
50	7.5	1.70

Fig. 5.6 : Effect of concentration on breakthrough of toluene over ACF (W = 5 g, Q_{N2}= 0.5 slpm = 0.5 slpm, T_{bed} = 50°C)		
Concentration (ppm)	b (1/kPa)	$C_{s\mu}$ (mmol/gm)
2000	45.0	0.49
4000	25.0	0.90
6000	13.9	1.14
10000	7.5	1.70

Table 5.4: Sips isotherm parameters for various experimental Conditions

(Sample # ACF-Type2, N = 1.0)

Sample	S. No.	VOC inlet concentration (ppm)	Breakthrough time (min)	Total adsorption time (min)
ACF-Type 1 (Procured locally)	1	2000	5	70
	2	4000	6	65
	3	6000	6	52
	4	10000	7	40
ACF-Type 2 (Imported)	5	2000	12	80
	6	4000	12	62
	7	6000	10	60
	8	10000	9	50

Table 5.5: Breakthrough time and total adsorption time of two different type of ACF samples at different VOC inlet concentration levels.

Concentration (ppm)	K (m^3/mol)	
	ACF (Type-1 sample) (Procured locally)	ACF (Type-2 sample) (Imported)
2000	61.79	120.84
4000	34.91	67.14
6000	32.22	37.32
10000	25.60	20.14

Table 5.6: Adsorption equilibrium constant at various VOC inlet concentration Levels

S.No	Flow rate (slpm)	Breakthrough Time (min)	Total Adsorption Time (min)
1	0.2	20	55
2	0.5	5	45
3	1.0	3	14

Table 5.7: Breakthrough time and total adsorption time at various gas flow rates

S.No	Adsorbent amount (gm)	Breakthrough Time (min)	Total Adsorption Time (min)
1	3	~ 0	30
2	5	5	40
3	9	16	60

Table 5.8: Breakthrough time and total adsorption time at different amounts of adsorbent

S. No	Temperature (^{0}C)	Concentration (ppm)	Flow Rate (slpm)	Wt (gm)	Superficial Velocity (m/s) x 10^3	Reynolds Number X 10^5	Schmidt Number	Mass transfer coefficient (m/s)	Effective Diffusivity (m^2/s) x 10^7	Dispersion Coefficient x 10^4 (m/s)	Sherwood Number
1	35	10000	0.5	5	1.17	4.14	1.38	41.241	1.11	2.925	2.00287
2	40	10000	0.5	5	1.20	4.14	1.40	41.242	1.12	2.925	2.00288
3	50	10000	0.5	5	1.23	4.14	1.45	41.242	1.15	2.925	2.00291
4	50	2000	0.5	5	1.23	4.14	1.45	41.242	1.14	2.925	2.00291
5	50	4000	0.5	5	1.23	4.14	1.45	41.242	1.14	2.925	2.00291
6	50	6000	0.5	5	1.23	4.14	1.44	41.242	1.14	2.925	2.00290
7	50	10000	0.2	5	0.045	1.65	1.45	41.217	1.14	2.925	2.00160
8	50	10000	1.0	5	2.47	8.28	1.45	41.273	1.14	2.925	2.00440
9	50	10000	0.5	3	1.23	4.14	1.45	41.242	1.14	2.288	2.00291
10	50	10000	0.5	9	1.2	4.14	1.45	41.242	1.14	2.925	2.00291

Table 5.9: Various operating parameters for model predictions for adsorption of toluene on ACF (Type-1 sample)
(Fiber diameter = 4.6 x 10^{-7} m, Pore radius = 3.0 x 10^{-9} m, Molecular diffusivity = 9.47 x 10^{-6} m^2/s)

61

CHAPTER 6

CONCLUSIONS AND RECOMMENDATIONS

The various conclusions that can be drawn from this study are summarized as follows:

1. The experimental results revealed that activated carbon fiber is a potential adsorbent for capturing VOCs at low concentration levels, due to its high BET surface area and micropore volume.

2. A bed temperature of 50 ^{0}C was found to be most favorable for capturing toluene vapor from a nitrogen stream in terms of longer breakthrough and adsorption times. The dynamic adsorption experiments carried out below and above this temperature resulted in smaller breakthrough and adsorption times.

3. Under the existing experimental conditions (T~ 35–50 ^{o}C) the heats of adsorptions were found to be 2.06 and 1.02 kc/mol for Type-1 and Type-2 ACF samples, respectively.

4. The breakthrough time during adsorption was observed to considerably decrease with increase in the concentration levels suggesting utility of the adsorption method for controlling VOC from gaseous effluent at ppm and sub-ppm levels. For example, the total adsorption time was found to increase from 40 to 70 min as the concentration level wss decreased from 10000 to 2000 ppm.

5. The commercially obtained ACF was shown to exhibit greater adsorption for VOC than granular activated carbon under identical operating conditions. This was attributed due to higher BET surface area of ACF (~1200 m^2/g) in comparison with that for GAC (~600 m^2/g).

6. Adsorption by ACF in the packed form was found to be more effective than that by the ACF wrapped over the perforated teflon reactor under the identical operating conditions (equal amount of adsorbent weight, temperature, concentration and flow rate). However, the ease of regeneration of saturated/equilibrated ACF by electrical heating in the case of ACF wrapped over the reactor was the main reason for using such type of arrangement over packed bed reactor.

7. Under existing operating conditions the ACF sample was regenerated approximately 25-30 times between two subsequent adsorption experiments, without exhibiting any degradation in its adsorption performance (breakthrough time).

8. A mathematical modeling for the prediction of breakthrough curve was developed based on three governing equations: (1) the species balance of the component in the

perforated bed, (2) species balance inside the pores of the fiber, and (3) adsorption/desorption rates within the pores. The Sips isotherm was found appropriate in explaining adsorption/desorption behavior of toluene on ACF. The experimental and model predicted results were found to be in good agreement within the experimental and computational error.

9. The fiber diameter being very small, the mass transfer coefficient in the bed was calculated to be very large at 41.24 m/s, even at small particle Reynolds number of 4.14 x 10^{-5}. This suggests that the resistance to the gas film mass transfer coefficient was negligible and the adsorption became independent of the film resistance.

Scope of future study:

The following recommendations are made to carry out further studies:

1. Studies on the removal of some other toxic VOCs (such as benzene, xylene, dimethylchloride, and trichloroethylene) and other gaseous pollutants like NO_x (NO & NO_2), SO_2, CO may be carried out on ACF or with other types of adsorbent materials like carbon molecular sieves (CMS), activated charcoal and zeolite.

2. Separate research studies may be carried out on the physical and chemical treatments required in carbonization and activation of raw fibers to enhance the BET surface area, pore size and to modify the surface functional groups which are responsible for the adsorption of various gaseous pollutants.

3. On theoretical sides, efforts can be made to find out a suitable correlation for the radial dispersion coefficient to achieve more accurate model predictive results.

Bibliography

Bird, R.B., W.E. Stewart, and E.N. Lightfoot, *Transport Phenomena*, Wiley, New York, NY (1960).

Cal, M.P., M.J. Rood, and S. M. Larson, Cal, M.P., "Experimental and modeled describing the adsorption of acetone and benzene onto activated carbons fibers" *Env. Prog.*, **13** (1994), 26

Cal, M.P., M.J. Rood, and S. M. Larson, "Removal of VOCs from humidified gas streams using activated carbon cloth", *Gas. Sep. purif*, **10** (1996), 117

Dasgupta, K., K. N. Rai, and N. Verma, "Breakthrough and sulphate conversion analysis during removal of sulphur-dioxide by calcium oxide sorbents", to be published in *Can. J. Chem.Eng.* (2003)

Duong, D.Do, *Adsorption Analysis Equilibria and Kinetics*, Imperial College Press (1998)

Duong, D.Do, and Ha D. Do, "A new adsorption isotherm for heterogeneous adsorbent based on the isoteric heat as a function of loading", *Chem. Eng. Sci.*, **52** (1997), 297

Do, D. D., A. Ahmadpour, and K. Wang, "Comparison of models on the prediction of binary equilibrium data of activated carbons", *AIChE J*, **44** (1998), 740

Donnet. J. B., Tong Kuan Wang, Jimmy C. M. Peng, and Serge Rebouillat, *Carbon Fibers*, 3rd ed., Marcel Dekker, Inc. Switzerland (1998)

Gupta. V. K., and N. Verma, "Removal of volatile organic compounds by cryogenic condensation followed by adsorption", *Chem. Eng. Sci.*, **57** (2002), 2679

Gupta. A., V. Gaur, and N. Verma, "Breakthrough analysis for adsorption of sulfur-dioxide over zeolites", to be published in *Chem. Eng. and Process.* (2003)

Kang, F., Z. H. Huang, K. M. Liang, and J. Hao, "Breakthrough of methyethylketone and benzene vapors in activated carbon fibers bed", to be published in *J Haz. Mat.* (2002)

Kim, et.al. "Adsorption equilibria of chlorinated organic solvents on to activated carbon", *Ind. Eng. Chem. Res.*, **37** (1998), 1422

McCabe, W.L., J.C. Smith, P. Harriott, *Unit Operations of Chemical Engineering*, 5th ed., McGraw Hill, New York, NY (1956).

Michio Inagaki, *New Carbons, control of structure and functions*, Elsevier Science Ltd., Oxford (2000)

Octave Levenspiel, *Chemical Reaction Engineering*, Wiley, New York, NY (1972)

Perry, R.H. and D. Green, *Perry's Chemical Engineers' Handbook*, 6th ed., McGraw-Hill, New York, NY (1984)

Robert, E. Treybal, *Mass Transfer Operations*, 3rd ed., McGraw Hill, New York, NY (2000).

Ruddy, E.N., and Carroll, L.A., "Select the best VOC control strategy", *Chem. Eng. Prog.*, **28** (1998).

Seinfeld, and Pandis, *Atmospheric Chemistry and Physics*, Wiley, New York, NY (1998).

Smith, J.M., *Chemical Engineering Kinetics*, Mc Graw-Hill, New-York, NY (1956)

Stenzel, M. H., and Fisher,J.L., "Use of Carbon Adsorption Process in Ground Water Treatment", *Env. Prog.*, **8** (1989), 257

Subrenat. A., J. N. Baleo, P. Le Cloirec, and P. E. Blanc, "Electrical behavior of activated carbon cloth heated by the joule effect: desorption application", *Carbon*, **39** (2001), 707.

Verma. N., V. Gaur, P. Dwivedi, and A. Sharma, "Comparative study of removal of Volatile Organic Compounds by Cryogenic Condensation and Adsorption by Activated Carbon Fiber", Proceedings of *9th APCChE Congress and CHEMECA 29th September to 3rd October 2002 Christ church, New Zealand.*

Yang, R.T., Gas Separation by Adsorption Processes, Imperial College Press, UK (1997)

Yun, J.H., Choi, D.K., and Kim, S. H., "Equilibria and dynamics for mixed vapors of BTX in an activated carbon bed", *AIChE J.*, **45** (1999), 751

APPENDIX

The following are the sample calculations for the parameters used in the model. The calculations have been done corresponding to the experimental conditions:

Superficial gas velocity:

gas flow rate = 0.5 slpm

$$Superficial\ gas\ velocity = \frac{(Flowrate)(R)(Temp)}{(22.4)(60)(pressure)(\pi DL_{Bed})} \qquad (A1)$$

where flow rate is in slpm

$$Superficial\ velocity = \frac{(0.5)(8.314)(323)}{(22.4)(60)(101325)(\pi \, x \, 0.0254 \, x \, 0.1)} = 1.23 x 10^{-3}\ \text{m/s}$$

Residence time:

$$Residence\ time\ of\ gas\ in\ the\ reactor = \frac{Bed\ thickness}{vel} \qquad (A2)$$

$$Residence\ time = \frac{1.27 x 10^{-3}}{1.23 x 10^{-3}} = 1.023\ \text{s}$$

Concentration of VOC in feed stream:

$$Concentration = \frac{(pressure)(mol\ fraction)}{(R)(Temperature)} \qquad (A3)$$

$$= \frac{(101325)(0.01)}{(8.314)(323)} = 0.2263\ \text{mol/m}^3$$

Bed porosity

Amount of sorbent = 5 gm

Solid density of the sorbent = 1200 kg/m^3

$$Actual\ volume\ of\ ACF\ sample = \frac{5 x 10^{-3}}{1200} = 4.166 x 10^{-6}\ \text{m}^3$$

Bulk volume of the adsorbent bed = $\pi \left[(0.014)^2 - (0.0127)^2\right] x \, 0.1 = 1.09 x 10^{-5}\ \text{m}^3$

$$Bed\ porosity\ \varepsilon = \frac{(1.09 x 10^{-5} - 4.166 x 10^{-6})}{1.09 x 10^{-5}} = 0.647 \qquad (A4)$$

Density of gas

$$\rho = \frac{(pressure)(mol.wt)}{(temperature)(R)}$$

$$= \frac{(101325)(92 \times 10^{-3})}{(8.314)(323)} = 1.056 \ \text{kg/m}^3 \tag{A5}$$

Reynolds number based on fiber diameter

$$\text{Re} = \frac{(gas\ density)(vel)(fiber\ diameter)}{(gas\ viscocity)} \tag{A6}$$

$$= \frac{(1.056)(1.23 \times 10^{-3})(4.6 \times 10^{-7})}{(1.45 \times 10^{-5})} = 4.14 \times 10^{-5}$$

Schmidt number

$$Sc = \frac{(gas\ viscosity)}{(gas\ density)(binary\ molecular\ diffusivity)} \tag{A7}$$

$$= \frac{1.45 \times 10^{-5}}{(1.056)(9.47 \times 10^{-6})} = 1.45$$

Dispersion co-efficient

The radial dispersion coefficient has been approximated by the following correlation for axial dispersion coefficient in a fixed bed (Yang, 1997):

$$D_R = \frac{D_m}{\varepsilon}(20 + 0.5 \, Sc \, \text{Re}) \tag{A8}$$

$$= \frac{9.47 \times 10^{-6}}{0.647} \left[20 + 0.5(1.45)(4.14 \times 10^{-5}) \right]$$

$$= \frac{9.47 \times 10^{-6}}{0.647} \left[20 + 0.5(1.45)(4.14 \times 10^{-5}) \right]$$

$$= 2.92 \times 10^{-4} \ \text{m/s}$$

Mass transfer coefficient:

The *mass transfer co-efficient* is calculated using the following correlations:

$$Sh = 2.0 + 1.1(Sc)^{0.33}(\text{Re})^{0.6} \tag{A9}$$

$$K_m = \frac{(2 + 1.1(Sc)^{0.33}(\mathrm{Re})^{0.6})(mol.diffusivity)}{(fiber\,diameter)}$$

$$= 41.24 \text{ m/s}$$

Calculation of diffusivity:

The effective diffusivity inside the pores is given by a combination of both Knudsen and molecular diffusion.

The *Knudsen diffusivity* is given by

$$D_K = \frac{2 \times r_p}{3}\left(\frac{8RT}{\pi M}\right)^{\frac{1}{2}} = 97 \times R_{pore}\left(\frac{T}{M}\right)^{\frac{1}{2}} \tag{A10}$$

where

R_{pore} = pore radius in m

M = Molecular weight in gm/gmmol

T = Temperature in K

D_k = Knudsen diffusion in m^2/s

The *Molecular diffusivity* for a binary gas mixture is given by the Wilke-Lee equation (Treybal, 1925):

$$D_m = \frac{10^{-4}(1.084 - 0.24(1/M_A + 1/M_B)^{0.5})T^{1.5}(1/M_A + 1/M_B)^{0.5}}{p_t(r_{AB})^2 f\left(\dfrac{kT}{\varepsilon_{AB}}\right)} \tag{A11}$$

Here,

D_m = Molecular diffusivity, m^2/s

T = Temperature in K

M_A, M_B = Molecular weight of the two interacting species (A: Toluene, B: N_2)

R_{AB} = molecular separation at collision, nm = $(r_A + r_B)/2$

ε_{AB} = energy of molecular attraction = $(\varepsilon_A \varepsilon_B)^{0.5}$

k = Boltzmann's constant

$f\left(\dfrac{kT}{\varepsilon_{AB}}\right)$ = collision function, a function of $\dfrac{kT}{\varepsilon_{AB}}$

$r_A = 0.602$ m, $\dfrac{\varepsilon_A}{k} = 464.398\,K$

$r_B = 0.380$ m, $\dfrac{\varepsilon_B}{k} = 71.4\,K$

$$\frac{\varepsilon_{AB}}{k} = (464.398 \times 71.4)^{0.5} = 182.09\,K$$

$$f\left(\frac{kT}{\varepsilon_{AB}}\right) = 0.56$$

$$r_{Toluene-N_2} = \frac{0.3798 + 0.602}{2} = 0.4909\ \text{nm}$$

$$(1/M_A + 1/M_B)^{0.5} = (1/92 + 1/28)^{0.5} = 0.2158$$

Substituting all the values in A(11)

$$D_m = \frac{10^{-4}(1.084 - 0.24(0.2158)^{0.5})(323)^{1.5}(0.2158)^{0.5}}{(101325)(0.4909)^2(0.56)} = 9.472 \times 10^{-6}\ \text{m}^2/\text{s}$$

The *combined diffusivity* contributed by both molecular and Knudsen diffusion is given by

$$\frac{1}{D} = \frac{1}{D_K} + \frac{1}{D_m} \tag{A12}$$

D = Diffusion co-efficient

The effective diffusivity inside the pores is found by using the formula

$$D_e = \frac{\alpha D}{\tau} \tag{A13}$$

where

α = Intrafiber void fraction

D = diffusivity co-efficient

τ = tortuosity factor

For micropore radius of 3.0×10^{-9} m

The Knudsen diffusivity $= (97)(3.0 \times 10^{-9})\left(\frac{323}{92}\right)^{0.5}$

$$= 5.45 \times 10^{-7}\ \text{m}^2/\text{s}$$

The Diffusion co-efficient is given by

$$\frac{1}{D} = \frac{1}{5.45 \times 10^{-7}} + \frac{1}{9.472 \times 10^{-6}}$$

$D = 5.15 \times 10^{-7} \ \text{m}^2/\text{s}$

The effective diffusivity is calculated as follows

$$D_e = \frac{D\alpha}{\tau}$$

where $\tau = 5$

$$D_e = \frac{(5.15 x 10^{-7}) x 0.7}{5} = 1.14 x 10^{-7} \ \text{m}^2/\text{s}$$

Adsorption and desorption rate constants:

From kinetic theory of gases adsorption rate constant, k_a is defined as:

$$k_a = s\left(\frac{RTx1000}{2\pi M}\right)^{0.5} \text{, where s is the sticking coefficient} \tag{A14}$$

Here, s = 1.0

$$k_a = \left(\frac{8.314 x 323 x 1000}{2 x \pi x 92}\right) = 68.15 \ \text{m/s}$$

Sips isotherm is given as follows (Do, 1998),

$$C_\mu = C_{\mu s} \frac{(bp)^{\frac{1}{N}}}{1+(bp)^{\frac{1}{N}}}; \text{ Here } P \text{ in } kPa \text{ and } C_{\mu s} \text{ is in } m - mol / g$$

Here C_s can be written as follows,

$$C_s = \left(\frac{C_\mu}{BET}\right) x 10^{-3} = C_{\mu s} \frac{(bp)^{\frac{1}{N}}}{1+(bp)^{\frac{1}{N}}} x \frac{10^{-3}}{BET}$$

Substituting p = C_pRT x 10^{-3} and comparing with equation (3.4) in theoretical analysis section we have ,

$$\frac{k_a}{k_d} = bRT \ x \ 10^{-3}$$

Here C_{smax} in equation (3.4) is given as follows,

$$C_{s\max} = \frac{C_{s\mu}}{BET} x 10^{-3}$$

*Desorption rate cons*tan*t,* $k_d = \dfrac{k_a}{bRT x 10^{-3}} = \dfrac{68.15}{12 x 8.314 x 323 x 10^{-3}} = 2.11 \ \text{mol/s-m}^2$

Input files for the code:

Oper:

0.5   0.01 1.0132×10^5 50.0   92.0   1.0 1×10^{-6} 25000

1. Flow rate of Gas (slpm)

2. Inlet Mol fraction of VOC

3. Pressure (N/m^2)

4. Initial Temperature (°C)

5. Molecular Weight,

6. Stick (sticking probability, to calculate rate constant for adsorption)

7. Initial mole fraction of voc

8. Final time step, s

Bed:

0.1 5.0 1200 0.55 0.5   700

1. Length of bed, m

2. Weight of the ACF, gm.

3. Solid density of the ACF, kg/m^3

4. Outer radius of the bed, inch.

5. Inner radius of the bed, inch.

6. Bulk density of ACF, kg/m^3

Iner:

1.45×10^{-5} 28.0

1. Viscosity of gas, pa-s

2. Molecular weight of gas

Sorbent:

3.0×10^{-9} 5.0 4.6×10^{-7} 1000.0

1. Radius of Pore, m

2. Tortuosity

3. Diameter of fiber, m

4. BET surface area, m^2/gm.

Vocc3:

8.5   0.95   1.0 9.472×10^{-6}

----

            toluene

1. bp

2. Csv (m.mol/gm)

3. fs

4. Molecular diffusivity, m^2/s

```fortran
C     Last change: I   28 Jan 2003   3:51 pm
*     D03PCF Example Program Text
*     Mark 15 Release. NAG Copyright 1991.
C     Last change: I   26 May 100   9:31 pm


C*********************************************************

*     .. Parameters ..
      INTEGER       NOUT
      PARAMETER     (NOUT=6)
      INTEGER       NPDE, NPTS, INTPTS, ITYPE, NEQN, NIW, NWK, NW
      PARAMETER (NPDE=3,NPTS=60000,INTPTS=6,ITYPE=1,NEQN=NPDE*NPTS,
     +          NIW=NEQN+24,NWK=(10+6*NPDE)*NEQN,
     +          NW=NWK+(21+3*NPDE)*NPDE+7*NPTS+54)
*     .. Scalars in Common ..

*     .. Local Scalars ..
      DOUBLE PRECISION ACC, HX,  PIBY2, TOUT, TS,ALPHA
      INTEGER       I, IFAIL, IND, IT, ITASK, ITRACE, M
*     .. Local Arrays ..
      DOUBLE PRECISION U(NPDE,NPTS), UOUT(NPDE,INTPTS,ITYPE), W(NW),
     +          X(NPTS), XOUT(INTPTS)
      DOUBLE PRECISION Cgf,cgi,Csmax,adcet,Fmass,outrad,innrad,ftime,
     +          Volflow,Eps,Lbed,surarea,fa,Rpore,Cfs,diaf,Pvoid,
     +          Deff,Vmf,Diff,bp,csv,temp,dia,Dz,yi,wfib,denf,res,
     +          Gden,dens,Cpg,Cps,Ya,pi,aprime,Vel,esa,Vo,bden,
     +          Vmw,stick,Rcons, AS,BS,CS,DS,ES,GS,FS,decet,aec,HS



      INTEGER       IW(NIW)
*     .. External Functions ..
      DOUBLE PRECISION X01AAF
      EXTERNAL      X01AAF
*     .. External Subroutines ..
      EXTERNAL      BNDARY, D03PCF, PDEDEF, UINIT!D03PZF
*     .. Intrinsic Functions ..
      INTRINSIC     SIN
*     .. Common blocks..

      COMMON        /VBLE/ALPHA
      COMMON/prop/Cgf,cgi,Csmax,Fmass,outrad,innrad,Volflow,Eps,
     1 Lbed,surarea,fa,Rpore,Cfs,diaf,Pvoid,aprime,
     2 Deff,Vmf,Diff,bp,csv,temp,dia,Dz,yi,Vel,esa
      COMMON/prop1/Gden,dens,Cpg,Cps
      COMMON/prop2/Vmw,stick,pi,Rcons
      COMMON/prop3/decet,aec,adcet
      COMMON/Prop4/AS,BS,CS,DS,ES,GS,FS,HS

      OPEN(UNIT=1,FILE="c:\deba\oper.txt",STATUS="UNKNOWN")
      OPEN(UNIT=2,FILE="c:\deba\bed.txt",STATUS="UNKNOWN")
      OPEN(UNIT=3,FILE="c:\deba\iner.txt",STATUS="Unknown")
      OPEN(UNIT=4,FILE="c:\deba\sorbent.txt",STATUS="UNKNOWN")
      OPEN(UNIT=5,FILE="c:\deba\vocc3.txt",STATUS="UNKNOWN")
      OPEN(UNIT=8,FILE="c:\deba\adsorb1.txt",STATUS="UNKNOWN")
      OPEN(UNIT=9,FILE="c:\deba\adsorb2.txt",STATUS="UNKNOWN")
      OPEN(UNIT=10,FILE="c:\deba\adsorb3.txt",STATUS=
     1 "UNKNOWN")
```

```fortran
      OPEN(UNIT=11,FILE="c:\deba\adsorb4.txt",STATUS=
1    "UNKNOWN")

*     .. Executable S

      READ(1,*) volflow,VMF,Pres,temp,Vmw,stick,yi
      WRITE(11,*)"volflow,VMF,Pres,temp,Vmw,stick,yi"
      WRITE(11,*)volflow,VMF,Pres,temp,Vmw,stick,yi
      READ(2,*) Lbed,wfib,denf, outrad,innrad,bden
      WRITE(11,*)"Lbed,wfib,denf,outrad,innrad,bden "
      WRITE(11,*) Lbed,wfib,denf,outrad,innrad,bden
      READ(3,*) Gvis,Gmw
      WRITE(11,*)"Gvis,Gmw"
      WRITE(11,*) Gvis,Gmw
      READ(4,*)Rpore,tor,diaf,surarea
      WRITE(11,*)"Rpore,tor,diaf,surarea"
      WRITE(11,*)Rpore,tor,diaf,surarea
      READ(5,*) bp,Csv,fa,Diff
      WRITE(11,*) "bp,Csv,fa,Diff"
      WRITE(11,*)bp,Csv,fa,Diff
      temp=temp+273.0  ! temperature,k
      rcons=8.314   !gas conbstant,(N/m2)(m3)/mol.k
      PI=4.0D0*ATAN(1.0e0)
      dia=2.0*innrad ! inch
      dia=dia*2.54e-2 !dia of bed,inch to meter
      outrad=outrad*2.54e-2 !dia of bed,inch to meter
      innrad=innrad*2.54e-2 !dia of bed,inch to meter
      Vo=PI*(outrad**2-innrad**2)*Lbed ! Bulk volume of the adsorbent bed, m3
      eps=(Vo-wfib/(denf*1000.0))/Vo ! Bed porosity
      pvoid=surarea*rpore*bden*1000.0/2.0 ! intrafiber porosity, dimensionless
      aprime=surarea*denf*1000.0 ! Total adsorption surface area per unit volume of fiber,m
      Cgi=pres*yi/(Rcons*temp)  !Initial conc. moles/m3
      Vel=Volflow*Rcons*Temp/(22.4*60.0*Pres*PI*Dia*Lbed) !superficial gas Velocity,m/s
      Gden=Pres*Gmw*0.001/(Rcons*Temp) !Gas density,kg/m3
      Re=Gden*Vel*diaf/Gvis   !Reynolds Number
      sc=gvis/(Gden*Diff) !schmidt number
      Fmass=Diff/diaf*(2.0+1.1*(Sc)**0.333*(Re)**0.6)   !Mass Transfer coefficient,m/s
      pin=pres*VMF    !partial pressure,pa
      Cgf=Pin/(Rcons*Temp)    !inlet conc. moles/m3
      Dk=97.0*Rpore*(Temp/Vmw)**0.5 !Knudsen diffusivity,m2/s
      Dz=Diff/eps*(20.0+0.5*Sc*Re) !axial dispersion coefficient, m2/s

      Deff=Dk*(Pvoid/tor) !m2/s, effective diffusivity inside the pores
      adcet=stick*(rcons*1.0e3*Temp/(2.0*PI*Vmw))**0.5 !adsorption coefficient, m/s
      decet=adcet/(bp*Rcons*Temp*1.0e-3) !desorption coefficient,  moles/s.m2
      aec=adcet/decet            !adsorption equilibrium constant
      esa=4.0/diaf ! external surface area per unit volume of fiber,1/m
      Csmax=Csv*1.0/surarea*1.0e-3   !moles adsorbed/BET area (sqm),Sips equation para
      AS=innrad/(outrad-innrad)  !coefficient of the governing equation
      Ya=Volflow*1.0e-3/(2.0*pi*Vel*60.0)!intermediate coefficient of the governing equation
      BS= Ya*(1.0/(outrad-innrad))**2 !coefficient of the governing equation
      CS=(Dz/(outrad-innrad)**2)*(Lbed/Vel) !coefficient of the governing equation
      DS=((1.0-Eps)/Eps)*Fmass*(Lbed/Vel)*esa !coefficient of the governing equation
      ES= 6.0/(diaf*Pvoid)*Fmass*(Lbed/Vel)!coefficient of the governing equation
      FS=(aprime/Pvoid)*(Csmax/Cgf) !coefficient of the governing equation
      GS=(adcet*Lbed*Cgf)/(Vel*Csmax)
      HS= (decet*Lbed)/(Vel*Csmax)
```

```fortran
      res=Lbed/Vel ! sec

      write(11,*) "temp=",temp        !temperature,k
      write(11,*) "dia=",dia       !dia of the bed,m
      write(11,*) "PI=",PI
      write(11,*) "Cgi=",Cgi        !initial concentration of voc,mol/m3
      write(11,*) "Vel=",vel        !superficial gas Velocity,m/s
      write(11,*) "Gden=",Gden        !gas density,kg/m3
      write(11,*) " Re=",Re         !Reynolds Number
      write(11,*) "sc=",sc          !schmidt number
      write(11,*) "Fmass=",Fmass     !mass transfer coefficient,m/s
      write(11,*) " pin=", pin       !partial pressure,pa
      write(11,*) "Cgf=",Cgf        !feed concentration of voc,mol/m3
      write(11,*) "Dk=",Dk          !Knudsen diffusivity,m2/s
      write(11,*) "Deff=",Deff       !m2/s, effective diffusivity inside the pores
      write(11,*) "Dz=",Dz          !axial dispersion coefficient
      write(11,*) "adcet=",adcet     !adsorption coefficient,m/s
      write(11,*) "decet=",decet      !desorption  coefficient, moles/s.m2
      write(11,*) "aec=",aec        !adsorption equilibrium constant
      write(11,*) "esa=",esa        ! external surface area per unit volume of fiber,1/m
      write(11,*) "Csmax=",Csmax
      write(11,*) "AS=",AS
      write(11,*) "Ya=",Ya      .
      write(11,*) "BS=",BS
      write(11,*) "CS=",CS
      write(11,*) "DS=",DS
      write(11,*) "ES=",ES
      write(11,*) "FS=",FS
      write(11,*) "GS=",GS
      write(11,*) "HS=",HS
      write(11,*) "eps=",eps !Bed porosity
      WRITE(11,*)"aprime=",aprime !Adsorption surface area per unit volume of fiber
      WRITE(11,*)"alpha=",pvoid  ! Intrafiber void fraction
      write(11,*) "res=",res


*  .. Data statements ..
      DATA        XOUT(1)/0.0e+0/, XOUT(2)/0.40e+0/,
     +            XOUT(3)/0.6e+0/, XOUT(4)/0.8e+0/,
     +            XOUT(5)/0.9e+0/, XOUT(6)/1.0e+0/
*

      ACC = 1.0e-4
      M = 1
      ITRACE =0
      ALPHA = 1.0e0
   .  IND = 0
      ITASK = 1
*
*     Set spatial mesh points
*
      PIBY2 = 0.5e0*X01AAF(PI)
      HX = PIBY2/(NPTS-1)
      HX=1.0/(npts-1)
      X(1) = 0.0e0
      X(NPTS) = 1.0e0
      DO  I = 2, NPTS - 1
      X(I)= SIN(HX*(I-1))
```

```fortran
          X(I) = HX*(I-1)
          enddo
*
*     Set initial conditions
*
      TS = 0.0e0
      TOUT =0.00001
      WRITE (11,99999) ACC, ALPHA
      WRITE (11,99998)(XOUT(I),I=1,6)
*
*     Set the initial values

      CALL UINIT(U,X,NPTS)
      DO IT = 1,500
                        ! IF(tout*res.ge.ftime)GO to 111
        IFAIL = -1
        TOUT=TOUT+0.2

      CALL D03PCF(NPDE,M,TS,TOUT,PDEDEF,BNDARY,U,NPTS,X,ACC,W,NW,IW,
     +          NIW,ITASK,ITRACE,IND,IFAIL)

*     Interpolate at required spatial points
*     CALL D03PZF(NPDE,M,U,NPTS,X,XOUT,INTPTS,ITYPE,UOUT,IFAIL)
      WRITE(10,99996)TOUT*res/60.0,U(1,NPTS/4),U(1,NPTS/2), U(1,NPTS)
      enddo
*
*     Print integration statistics

      WRITE (11,99997) IW(1), IW(2), IW(3), IW(5)
      STOP

99999 FORMAT (//' Accuracy requirement = ',e12.5,/' Parameter ALPHA =',
     +        '      ',e12.3,/)
99998 FORMAT ('   T / X ',6F8.4,/)
99997 FORMAT (' Number of integration steps in time            ',
     +        I4,/' Number of residual evaluations of resulting ODE sys',
     +        'tem',I4,/' Number of Jacobian evaluations            ',
     +        '         ',I4,/' Number of iterations of nonlinear solve',
     +        'r           ',I4,/)
99996 FORMAT (1x,F14.6,3(1x,F14.6))

      END

      SUBROUTINE UINIT(U,X,NPTS)
*     Routine for PDE initial conditon
*     .. Scalar Arguments ..

      INTEGER     NPTS
*     .. Array Arguments ..
      DOUBLE PRECISION U(3,NPTS), X(NPTS)
      DOUBLE PRECISION Cgf,cgi,Csmax,adcet,Fmass,outrad,innrad,
     +        Volflow,Eps,Lbed,surarea,fa,Rpore,Cfs,diaf,Pvoid,
     +        Deff,Vmf,Diff,bp,csv,temp,dia,Dz,yi,
     +        Gden,dens,Cpg,Cps,Ya,pi,aprime,Vel,esa,
     +        Vmw,stick,Rcons,AS,BS,CS,DS,ES,GS,FS,decet,aec,HS

*     .. Scalars in Common ..
```

```fortran
*     .. Local Scalars ..
      INTEGER       I
*     .. Scalars in Common ..
      DOUBLE PRECISION  ALPHA

*     .. Common blocks ..

      COMMON        /VBLE/ALPHA
      COMMON/prop/Cgf,cgi,Csmax,Fmass,outrad,innrad,Volflow,Eps,
     1 Lbed,surarea,fa,Rpore,Cfs,diaf,Pvoid,aprime,
     2 Deff,Vmf,Diff,bp,csv,temp,dia,Dz,yi,Vel,esa
      COMMON/prop1/Gden,dens,Cpg,Cps
      COMMON/prop2/Vmw,stick,pi,Rcons
      COMMON/prop3/decet,aec,adcet
      COMMON/Prop4/AS,BS,CS,DS,ES,GS,FS,HS


*     .. Executable Statements ..
      DO 20 I =1,NPTS
        U(1,I)=Cgi/Cgf
        U(2,I)=Cgi/Cgf
        U(3,I)=(aec*Cgi)**(1.0/fa)/((aec*Cgi)**(1.0/fa)+1.0)

   20 CONTINUE

      RETURN
      END

      SUBROUTINE PDEDEF(NPDE,T,X,U,DUDX,P,Q,R,IRES)
*     .. Scalar Arguments ..
      DOUBLE PRECISION  T, X
      INTEGER       IRES, NPDE
*     .. Array Arguments ..
      DOUBLE PRECISION  DUDX(NPDE), P(NPDE,NPDE), Q(NPDE), R(NPDE),
     +        U(NPDE)
      DOUBLE PRECISION Cgf,cgi,Csmax,adcet,Fmass,outrad,innrad,
     +        Volflow,Eps,Lbed,surarea,fa,Rpore,Cfs,diaf,Pvoid,
     +        Deff,Vmf,Diff,bp,csv,temp,dia,Dz,yi,
     +        Gden,dens,Cpg,Cps,Ya,pi,aprime,Vel,esa,
     +        Vmw,stick,Rcons, AS,BS,CS,DS,ES,GS,FS,decet,aec,HS

*     .. Scalars in Common ..
      DOUBLE PRECISION  ALPHA

*     .. Common blocks ..

      COMMON        /VBLE/ALPHA
      COMMON/prop/Cgf,cgi,Csmax,Fmass,outrad,innrad,Volflow,Eps,
     1 Lbed,surarea,fa,Rpore,Cfs,diaf,Pvoid,aprime,
     2 Deff,Vmf,Diff,bp,csv,temp,dia,Dz,yi,Vel,esa
      COMMON/prop1/Gden,dens,Cpg,Cps
      COMMON/prop2/Vmw,stick,pi,Rcons
      COMMON/prop3/decet,aec,adcet
      COMMON/Prop4/AS,BS,CS,DS,ES,GS,FS,HS
```

```fortran
*      .. Executable Statements ..

       Cfs= (U(1)*Fmass+10.0/diaf*Deff*U(2))/(Fmass+10.0/diaf*Deff)
       Q(1)=BS/(CS*X)*DUDX(1)+ DS/(CS*X)*(X+AS)*(U(1)-Cfs)
       Q(2)= -ES*(U(1)-Cfs)
       Q(3)= -GS*U(2)*(1-U(3))**fa+HS*U(3)**fa
       R(1) =(1+AS/X)*DUDX(1)
       R(2) =0.0e+0
       R(3) =0.0e+0
       P(1,1) =(X+AS)/(CS*X)
       P(1,2) = 0.0e+0
       P(1,3) = 0.0e+0
       P(2,1) = 0.0e+0
       P(2,2) =1.0e0
       P(2,3) =FS
       P(3,1) = 0.0e+0
       P(3,2) = 0.0e+0
       P(3,3) = 1.0e0


       RETURN
       END
*
       SUBROUTINE BNDARY(NPDE,T,U,UX,IBND,BETA,GAMMA,IRES)
*      .. Scalar Arguments ..
       DOUBLE PRECISION  ALPHA
       DOUBLE PRECISION  T
       INTEGER           IBND, IRES, NPDE
*      .. Array Arguments ..
       DOUBLE PRECISION  BETA(NPDE), GAMMA(NPDE), U(NPDE), UX(NPDE)
       DOUBLE PRECISION Cgf,cgi,Csmax,adcet,Fmass,outrad,innrad,
      +          Volflow,Eps,Lbed,surarea,fa,Rpore,Cfs,diaf,Pvoid,
      +          Deff,Vmf,Diff,bp,csv,temp,dia,Dz,yi,
      +          Gden,dens,Cpg,Cps,Ya,pi,aprime,Vel,esa,
      +          Vmw,stick,Rcons, AS,BS,CS,DS,ES,GS,FS,decet,aec,HS

*      .. Common blocks ..
       COMMON          /VBLE/ALPHA
       COMMON/prop/Cgf,cgi,Csmax,Fmass,outrad,innrad,Volflow,Eps,
      1 Lbed,surarea,fa,Rpore,Cfs,diaf,Pvoid,aprime,Dz,yi,
      2 Deff,Vmf,Diff,bp,csv,temp,dia, Vel,esa
       COMMON/prop1/Gden,dens,Cpg,Cps
       COMMON/prop2/Vmw,stick,pi,Rcons
       COMMON/prop3/decet,aec,adcet
       COMMON/Prop4/AS,BS,CS,DS,ES,GS,FS,HS

*      .. Executable Statements ..

       IF (IBND.EQ.0) THEN
       BETA(1) = 0.0
       BETA(2) = 0.0
       BETA(3) = 0.0
       GAMMA(1) = U(1)-1.0
       GAMMA(2) = U(2)-1.0
       GAMMA(3) = U(3)-(aec*Cgf)**(1.0/fa)/((aec*Cgf)**(1.0/fa)+1.0)

       ELSE
```

```
      BETA(1) = 1.0e+0
      BETA(2) = 1.0e+0
      BETA(3) = 1.0e+0
      GAMMA(1) =0.0e+0
      GAMMA(2) =0.0e+0
      GAMMA(3) =0.0e+0


   END IF
   RETURN
   END
```